ISTANBUL TECHNICAL UNIVERSITY ★ GRADUATE SCHOOL

INVESTIGATION OF THERMAL PROPAGATION IN ELECTRIC VEHICLE HIGH VOLTAGE BATTERIES

M.Sc. THESIS

Kadir ARAS

Energy Science and Technology Division

Energy Science and Technology Programme

JUNE 2023

ISTANBUL TECHNICAL UNIVERSITY ★ GRADUATE SCHOOL

INVESTIGATION OF THERMAL PROPAGATION IN ELECTRIC VEHICLE HIGH VOLTAGE BATTERIES

M.Sc. THESIS

Kadir ARAS
(301191052)

Energy Science and Technology Division

Energy Science and Technology Programme

Thesis Advisor: Prof. Dr. Nilgün KARATEPE YAVUZ

JUNE 2023

İSTANBUL TEKNİK ÜNİVERSİTESİ ★ LİSANSÜSTÜ EĞİTİM ENSTİTÜSÜ

ELEKTRİKLİ ARAÇ YÜKSEK GERİLİM BATARYALARINDA ISIL YAYILIM ARAŞTIRMASI

YÜKSEK LİSANS TEZİ

Kadir ARAS
(301191052)

Enerji Bilim ve Teknoloji Anabilim Dalı

Enerji Bilim ve Teknoloji Programı

Tez Danışmanı: Prof. Dr. Nilgün KARATEPE YAVUZ

HAZİRAN 2023

Kadir ARAS, a M.Sc. student of İTU Graduate School student ID 301191052 successfully defended the thesis entitled "INVESTIGATION OF THERMAL PROPAGATION IN ELECTRIC VEHICLE HIGH VOLTAGE BATTERIES", which he prepared after fulfilling the requirements specified in the associated legislations, before the jury whose signatures are below.

Thesis Advisor :	**Prof. Dr. Nilgün KARATEPE YAVUZ** Istanbul Technical University	.....
Jury Members :	**Prof. Dr. Üner ÇOLAK** Istanbul Technical University	.....
	Assoc. Prof. Dr. Metin GENÇTEN Yıldız Technical University	.....

Date of Submission : 24 May 2023
Date of Defense : 19 June 2023

To my family and friends,

FOREWORD

First of all, I would like to thank my advisor Prof. Dr. Nilgün K. YAVUZ for agreeing to work with me and supporting me through the process.

I would like to give my gratitude to Halil Sadi HAMUT, Burak EVYAPAN, Oğuz TORUNOĞLU, Selim YILMAZ, Orçun KARADENİZ, Gökhan ERDOĞAN, Anıl DEMİRKESEN and Ümit Emre ERDOĞAN for their great support. They are outstanding team mates.

June 2023

Kadir ARAS
(Electrical Engineer)

TABLE OF CONTENTS

Page

ABBREVIATIONS

AC : Alternative Current
BMS : Battery Management System
CFD : Compression Force Displacement
DMC : Dimethyl Carbonate
EIS : Irreversible Capacity Loss
EC : Ethylene Carbonate
EV : Electric Vehicles
G : Graphite
HV : High Voltage
LCO : Lithium Cobalt Oxide
LFP : Lithium Iron Phosphate
LIBs : Lithium-Ion Batteries
NiCad : Nickel Cadmium
NMC : Lithium Nickel Manganese Cobalt Oxide
PP : Polypropylene
PE : Polyethylene
SEI : Solid Electrolyte Interphase
SOC : State of Charge
TP : Thermal Propagation
TR : Thermal Runaway
UL : Underwriters Laboratories
UNECE : The United Nations Economic Commission for Europe
UNGTR : The United Nations Global Technical Regulations
YG : Yüksek Gerilim

SYMBOLS

A	**:** Ampere
BTU/hr-ft-°F	**:** BTU per hour per foot-degree Fahrenheit
°C	**:** Celsius Degree
g/cm^3	**:** Gram per cubic centimeter
mm	**:** Millimeter
V	**:** Volt
W	**:** Watt
W/mK	**:** Watts per meter-kelvin

LIST OF TABLES

Page

LIST OF FIGURES

Page

INVESTIGATION OF THERMAL PROPAGATION IN ELECTRIC VEHICLE HIGH VOLTAGE BATTERIES

SUMMARY

Understanding the Li-ion battery, which is essentially driving the industry, is important given the expansion of the vehicle electrification market, rising environmental and governmental laws, urbanization trends, rising fuel prices, and a developing client market. The increasing demand for electric vehicles (EVs) has released the need for efficient and reliable energy storage solutions. Lithium-ion batteries have emerged as a leading technology due to their high energy density, long cycle life, and lightweight design. The effort to save modern society from energy crises and environmental pollution relies on clean energy.

In this study, a brief explanation of lithium-ion materials was given including cathode materials, anode materials, electrolytes, and separators. The cathode materials, such as lithium cobalt oxide (LCO), lithium nickel manganese cobalt oxide (NMC), and lithium iron phosphate (LFP), significantly impact battery performance by influencing energy density, power capability, and safety considerations. On the other hand, anode materials such as graphite and silicon play a crucial role in capacity and rate capabilities, and the thesis gives the characteristics, challenges, and opportunities associated with different anode materials.

Furthermore, the study delves into the underlying mechanisms behind ageing phenomena. Factors such as side reactions, cycling, storage conditions and contamination contribute to battery ageing. As a result of ageing, capacity fades and impedance increases.

Moreover, this thesis also addresses the thermal runaway (TR) mechanism which is a key safety concern in lithium-ion batteries. It explores the conditions that can lead to thermal runaway, such as overcharging, high temperature, and mechanical abuse. Various strategies to mitigate thermal runaway, including advanced cell designs, thermal management systems, protection systems and packaging are evaluated for their effectiveness in enhancing battery safety.

Foams are a key component in providing thermal management when building a high voltage (HV) battery pack module. Correct foam selection provides a better thermal management system, safer system, longer life cycle and easier module production. In the study, thermal propagation (TP) behavior in HV batteries was investigated and the effects of parameters such as thermal conductivity and compression force-displacement of three different foam materials on thermal dissipation were evaluated. After the determination of optimum foam by experiments, pack-level thermal propagation was tested and investigated. To optimize the TP duration, experiments were carried out and the effects of short circuits and pressure were examined through the tests. As a result, the precautions to be taken were determined and the importance of investigating thermal propagation in electric vehicle HV batteries was emphasized.

Keywords: Thermal propagation, lithium-ion batteries, electric vehicles.

ELEKTRİKLİ ARAÇ YÜKSEK GERİLİM BATARYALARINDA ISIL YAYILIM ARAŞTIRMASI

ÖZET

Elektrikli araçlar, çevre bilincinin artması ve hükümet politikalarındaki değişiklikler gibi etkenlerle birlikte hızla yayılan bir teknoloji olmuştur. Bu araçlar, geleneksel içten yanmalı motorlu araçlara kıyasla çeşitli avantajlara sahiptir. İlk olarak, elektrikli araçlar çevre dostudur. Sıfır veya düşük emisyonlu çalışmaları sayesinde hava kirliliğini ve sera gazı salınımını azaltır, iklim değişikliğiyle mücadelede önemli bir rol oynar. Ayrıca, enerji verimlilikleri daha yüksektir ve enerjiyi daha etkin bir şekilde kullanır. İçten yanmalı motorlara kıyasla enerji kayıplarını minimize ederek daha fazla mesafe kat eder. Aynı zamanda, elektrikli araçların işletme maliyetleri düşüktür. Elektrik enerjisinin yakıta kıyasla genellikle daha ucuz olması ve daha az bakım gerektirmesi, kullanıcılar için ekonomik bir avantaj sağlar. Bununla birlikte, elektrikli araçların bazı dezavantajları da vardır. Öncelikle, sınırlı menzil sorunu bulunmaktadır. Bir pil şarjıyla kat edilebilecek mesafe sınırlıdır ve uzun yolculuklarda veya şarj altyapısının yetersiz olduğu bölgelerde kullanıcılar için bir zorluk oluşturabilir. Şarj altyapısının henüz tam olarak gelişmemiş olması da bir diğer dezavantajdır. Şarj istasyonlarının sayısı ve yaygınlığı hala yetersiz olabilir. Ayrıca, elektrikli araçların şarj süreleri benzine veya dizele kıyasla daha uzun olabilir. Bu durum, acil durumlar veya uzun yolculuklar için planlama gerektirebilir. Son olarak, lityum-iyon pillerin ömrü sınırlıdır ve pil değiştirme veya geri dönüşüm süreçleri karmaşık ve maliyetli olabilir. Bununla birlikte, elektrikli araç teknolojilerindeki ilerlemeler ve altyapı iyileştirmeleriyle birlikte, bu dezavantajların azaltılması ve elektrikli araçların daha geniş bir kullanımının sağlanması beklenmektedir.

Elektrikli araç pazarının genişlemesi, artan çevre bilinci ve hükümet politikaları, kentleşme eğilimleri, yükselen yakıt fiyatları ve gelişen bir müşteri pazarı göz önüne alındığında, öne çıkan enerji depolama teknolojilerinden biri olan Li-ion pili anlamak önemlidir. Yüksek enerji yoğunlukları, lityum-iyon pilleri özellikle elektrikli araçlar için ideal bir seçenek haline getirir. Bu piller, küçük bir ağırlıkla büyük miktarda enerji depolayabilirler, böylece araçlara daha uzun menzil sağlarlar. Ayrıca, lityum-iyon pillerin uzun bir çevrim ömrü vardır, yani birçok şarj-deşarj döngüsüne dayanabilirler. Bu da pilin ömrünü uzatarak kullanıcılar için ekonomik bir seçenek olmasını sağlar. Lityum-iyon piller aynı zamanda hafiftir, bu da onları taşıması ve montajı kolay hale getirir. Elektrikli araçların yanı sıra, lityum-iyon piller güneş enerjisi ve rüzgar enerjisi gibi yenilenebilir enerji kaynaklarının depolanmasında da yaygın olarak kullanılmaktadır. Bu pillerin hafifliği ve kompakt tasarımı, enerji depolama sistemlerini daha verimli ve esnek hale getirir. Modern toplumun enerji krizleri ve çevre kirliliği gibi zorluklara karşı mücadele etme çabası, temiz enerjiye dayalı çözümlere yönelmeyi gerektirmektedir. Lityum-iyon piller, fosil yakıtlara bağımlılığı azaltarak ve karbon salınımını önemli ölçüde azaltarak sürdürülebilir enerji dönüşümüne önemli bir katkıda bulunabilir.

Bu çalışma, lityum iyon pillerinin temel yapı taşlarını oluşturan malzemeler hakkında önemli bilgiler sunmaktadır. Lityum iyon pilleri, katot malzemeleri, anot malzemeleri, elektrolitler ve separatörler gibi bir dizi malzemeden oluşur. Katot malzemeleri, pilin pozitif elektrodu olarak görev yapar ve lityum iyonlarını depolamak ve serbest bırakmak için kullanılır. Lityum kobalt oksit (LCO), lityum nikel manganez kobalt oksit (NMC) ve lityum demir fosfat (LFP) gibi çeşitli katot malzemeleri mevcuttur. Her bir malzemenin farklı enerji ve güç yoğunlukları, güvenlik özellikleri ve pil performansına etkisi bulunur. Örneğin, NMC yüksek enerji yoğunluğu sağlarken, LFP daha güvenli ve termal kararlılık sağlar. Katot malzemelerinin seçimi, pilin performansı, enerji yoğunluğu, döngü ömrü ve güvenlik açısından kritik bir öneme sahiptir. Anot malzemeleri, pilin negatif elektrodu olarak görev yapar ve lityum iyonlarının depolanması ve salınması için kullanılır. Anot malzemeleri, pilin kapasitesini etkileyen önemli faktörlerden biridir. Grafit genellikle yaygın bir anot malzemesi olarak kullanılırken, silikon gibi yüksek kapasiteli malzemeler de araştırılmaktadır. Ancak, silikon gibi yüksek kapasiteli malzemelerin kullanımı zorluklar da sunar. Silikon, genişlemeye ve büzülmeye yatkındır, bu da pilde yapısal hasara neden olabilir. Araştırmalar, daha verimli ve güvenilir anot malzemelerinin geliştirilmesi üzerine yoğunlaşmaktadır. Elektrolitler, lityum iyonlarının katot ve anot arasında hareket etmesini sağlar. Elektrolitler, iyon iletimini sağlamak için lityum tuzları ve organik çözücülerin kombinasyonunu içerir. Separatörler, katot ve anot arasında mekanik ve elektriksel olarak izolasyon sağlar. Separatörler, lityum iyonlarının geçişine izin verirken elektron geçişini engeller. Bu malzemelerin seçimi ve özellikleri, lityum iyon pillerin performansını, enerji yoğunluğunu, döngü ömrünü ve güvenliğini etkiler. Araştırmalar, yeni malzemelerin keşfi, malzeme tasarımlarının iyileştirilmesi ve pil teknolojilerinin geliştirilmesi üzerinde odaklanmaktadır. Bu sayede daha verimli, güvenilir ve güvenli lityum iyon piller geliştirilebilir.

Tez çalışması kapsamında, pillerin yaşlanma mekanizmaları detaylı bir şekilde incelenmiş ve bu sürecin anlaşılması için çeşitli faktörler göz önünde bulundurulmuştur. Pil yaşlanması, yan reaksiyonlar, çevrim ömrü, depolama koşulları ve kontaminasyon gibi çeşitli faktörlerin etkileşimiyle gerçekleşir. Yan reaksiyonlar, pildeki elektrokimyasal reaksiyonlardan kaynaklanan yan ürünlerin oluşumunu ifade eder. Bu yan ürünler, elektrotlar arasında birikerek pilin performansını olumsuz yönde etkiler. Örneğin, lityum-iyon pillerde, yan reaksiyonlar anotun üzerinde lityum metalinin oluşumuna neden olabilir ve bu da pilin kapasitesini azaltabilir. Çevrim ömrü, bir pilin tam şarj ve deşarj döngülerine dayanabilme kabiliyetini ifade eder. Her bir şarj-deşarj döngüsü, pilin elektrokimyasal reaksiyonlara bağlı olarak fiziksel ve kimyasal değişimler yaşamasına neden olur. Bu süreçte, aktif malzemelerin bozulması, elektrotların yıpranması ve elektrolitin etkinliğinin azalması gibi faktörler pilin yaşlanmasına katkıda bulunur. Çevrim ömrünün anlaşılması, pilin performansını ve ömrünü iyileştirmek için önemli bir adımdır. Depolama koşulları da pillerin yaşlanmasında önemli bir rol oynar. Uzun süreli depolama, pilin performansını olumsuz yönde etkileyebilir. Yüksek sıcaklık, nem, oksidasyon gibi faktörler, pilin kimyasal kararlılığını bozarak yaşlanmasını hızlandırabilir. Bu nedenle, pilin uzun süreli depolanması sırasında uygun sıcaklık ve nem koşullarının sağlanması önemlidir. Kontaminasyon, pilin içindeki bileşenlere yabancı maddelerin girmesi anlamına gelir. Bu yabancı maddeler, elektrotlarda paslanma, elektrolit ile etkileşim veya kimyasal reaksiyonlara neden olarak pilin performansını olumsuz etkiler. Kontaminasyonun azaltılması veya engellenmesi, pilin yaşlanma sürecini yavaşlatabilir ve performansını korumasına yardımcı olabilir. Bu faktörlerin bir araya gelmesi, pillerin yaşlanmasına ve performansının azalmasına yol açar. Bu nedenle, pil ömrünün ve performansının

iyileştirilmesi için yaşlanma mekanizmasının tam olarak anlaşılması önemlidir.Yaşlanma sonucu olarak pilin kapasitesi azalır ve empedansı artar.

Lityum iyon piller, sürekli olarak geliştirilen bir teknoloji olmakla birlikte, güvenlik endişeleri bu teknolojinin yaygın kullanımını sınırlamaktadır. Özellikle ısıl bozunum mekanizması, lityum iyon pillerin güvenliği üzerinde önemli bir etkiye sahiptir. Aşırı şarj, yüksek sıcaklık, mekanik hasar veya yanlış kullanım gibi durumlar, pilin iç yapısında anormal ısı birikimi ve tepkimelerin başlamasına yol açabilir. Isıl bozunumun önlenmesi ve pil güvenliğinin artırılması için çeşitli yöntemler ve stratejiler benimsenmektedir. Hücre tasarımında yapılan iyileştirmeler, pilin ısıl yayılımını kontrol etmeye yönelik adımları içerir. Termal yönetim sistemleri, pilin ısı dağılımını optimize ederken aşırı ısınma riskini azaltmaya yardımcı olur. Isıyı ileten malzemeler, ısı yayılımını artırabilirken soğutma sistemleri, pilin sıcaklığını düşürmeye yardımcı olur. Bunun yanı sıra, güvenlik önlemleri ve koruma sistemleri, lityum iyon pillerin güvenliğini artırmak için önemli bir rol oynamaktadır. Aşırı akım korumaları, aşırı şarjı önlemek ve pilin güvenli bir şekilde çalışmasını sağlamak için kullanılır. Aşırı sıcaklık durumunda otomatik kesme devreleri çalışarak pilin zarar görmesini önler. Aynı şekilde, kısa devre koruma sistemleri, pilde meydana gelebilecek kısa devreleri algılar ve güvenlik önlemlerini devreye sokar. Pil güvenliğini artırmak için yapılan çalışmalar, paketleme ve malzeme seçimine de odaklanmaktadır. Güvenli bir pil paketi, pil hücrelerini dış etkenlere karşı koruyan dayanıklı ve izole edici malzemelerle donatılmalıdır. Ayrıca, pil paketindeki gaz birikimini önlemek için basınç düzenleyiciler ve gaz tahliye valfleri gibi özellikler de bulunabilir. Bu bağlamda, pil güvenliğini artırmak için yapılan araştırma ve geliştirme çalışmaları devam etmektedir. Ayrıca, güvenlik standartlarının ve yönetmeliklerinin sürekli olarak gözden geçirilerek güncellenmesi, pil güvenliğini artırmak için önemli bir adımdır. Sonuç olarak, lityum iyon pillerin güvenliği, teknolojisinin daha da ilerlemesi ve yaygınlaşması için öncelikli bir konudur. Isıl bozunum mekanizması ve diğer güvenlik sorunlarına odaklanarak, pil güvenliği konusundaki bilgi ve teknoloji geliştirme çalışmaları devam etmektedir. Bu çabalar, lityum iyon pillerin güvenilirliğini artırmak ve daha geniş bir kullanım alanı yaratmak için önemli adımlar sağlayacaktır.

Bu tez kapsamında bir yüksek gerilim (YG) bataryanın ısıl yayılım performansını arttırmaya yönelik bir çalışma yapılmıştır. Elektrikli ve hibrit araçlarda kullanılan YG bataryalar genel olarak lityum-iyon hücreler, mekanik yapı ve modüller, ısıl sistem, batarya yönetim sistemi, elektrik sistemi ve koruma elemanları olmak üzere beş ana bileşenden oluşmaktadır. Modüller basit bir şekilde lityum iyon hücrelerden, köpüklerden, sensörlerden ve mekanik yapıdan oluşmaktadır. Bir yüksek gerilim (YG) batarya paketi modülü oluşturulurken ısıl yönetimi sağlamada köpükler temel bileşenlerden biridir. Doğru köpük seçimi, daha iyi bir ısıl yönetim sistemi, daha güvenli sistem, daha uzun ömür ve daha kolay modül üretimi sağlar. Tez çalışmasında, ilk olarak üç farklı köpük malzemenin, ısı iletkenliği, sıkıştırma kuvveti-yer değiştirme gibi parametrelerinin ısıl yayılmaya olan etkileri incelenmiştir. Öncelikle, gerçekleştirilen deneylerle ısıl bozunum tetikleme mekanızmasına karar verilmiş, ardından, üç köpük ile ısıl yayılım testleri yapılıp, en uygun köpük seçilmiştir. Daha sonra, bu modüllerden YG batarya paketi oluşturulmuş ve paket seviyesi termal yayılım testleri yapılmıştır. Sonuç olarak, ısıl yayılım süresini uzatmak için alınması gereken önlemler belirlenmiş ve termal yayılımın önemi vurgulanmıştır.

Anahtar Kelimeler: Isıl yayılım, lityum-iyon bataryalar, elektrikli araçlar.

1. INTRODUCTION

Global efforts to develop renewable energy sources and electrify a variety of businesses, including electric vehicles (EVs), portable devices, and renewable energy storage, have gathered substantial momentum in recent years. The creation of effective and dependable energy storage systems is required by this paradigm shift toward market electrification. Due to its high energy density, long cycle life, and lightweight construction, lithium-ion batteries have emerged as the best option among the numerous technologies now in use. To enhance their performance, safety, and general viability for market electrification, this thesis aims to investigate thermal propagation which is a key safety concern in lithium-ion batteries, focusing on module level design matter and pack level measures. Before experimental studies lithium-ion batteries, their cathode materials, anode materials, electrolytes, separators, ageing mechanisms, and thermal runaway mechanisms were explained [1].

The energy density, power capacity, and safety of lithium-ion batteries are greatly influenced by the materials used for their cathodes. Lithium cobalt oxide (LCO), lithium nickel manganese cobalt oxide (NMC), and lithium iron phosphate (LFP) are just a few examples of materials that have undergone substantial research and development [1]. Similarly, the anode materials used in lithium-ion batteries have a big impact on their ability to store and discharge energy. Due to its stability and cycle capability, graphite has historically been the main component of anodes. Alternative substances like silicon and lithium titanate oxide (LTO) have demonstrated promise in enhancing battery performance [2]. Battery performance, security, and stability are significantly influenced by electrolyte, which acts as a carrier for ionic conduction between the cathode and anode. Numerous battery properties are significantly influenced by the composition of the electrolyte, which includes the types of solvents, salts, and additions. The separator, in addition to the cathode, anode, and electrolyte, is an essential part of lithium-ion batteries. It serves as a physical barrier that allows ions to pass through while preventing short circuits between the cathode and anode. It

is essential to choose the right separator materials, taking into account elements like permeability, mechanical strength, and electrochemical stability [1].

For lithium-ion batteries to last longer and function better, it is crucial to understand how they age. Battery ageing is caused by elements like capacity decline, impedance growth, and adverse reactions. This thesis will give information about the underlying causes of ageing phenomena to illuminate mitigation techniques and boost battery performance over long cycles [3].

The thermal runaway mechanism in lithium-ion batteries poses a serious safety risk. Batteries may exhibit uncontrolled thermal runaway that results in catastrophic failures under certain circumstances, such as overcharging, extreme temperatures, or mechanical abuse. To create efficient safety measures and boost battery reliability, it is imperative to investigate the circumstances and mechanisms that lead to thermal runaways [4].

In this study, thermal propagation (TP) behavior in HV batteries was investigated and the effects of parameters such as thermal conductivity and compression force-displacement of three different foam materials on thermal dissipation were evaluated. After the determination of optimum foam by experiments, pack-level thermal propagation was tested and investigated. To optimize the TP duration, experiments were carried out and the effects of short circuits and pressure were examined through the tests. As a result, the precautions to be taken were determined and the importance of investigating thermal propagation in electric vehicle HV batteries was emphasized.

2. LITERATURE

2.1 Brief Explanation of Batteries

2.1.1 General overview

There are technical and economic limitations to the direct storage of electrical energy with electrolytic capacitors or superconducting coils. Therefore, the storage of electrical energy requires its conversion into another form of energy. It can be stored by converting to potential, kinetic, thermal or chemical energy.

A battery is a chemical device for the storage of electrical energy. The energy of chemical compounds in batteries acts as a storage medium and while discharged, the battery converts the chemical energy into electrical energy using an electrochemical reaction [5]. Even though the term “cell” is used for the basic electrochemical unit, the term “battery” is more widely accepted. Depending on the required output voltage or capacity, cells are connected in series, parallel or both. Two or more electrically joined cells are called a battery.

Mainly batteries are classified as primary (non-rechargeable) or secondary (rechargeable) batteries in terms of their reuseability. Regarding particular structures and/or designs, further classifications are also used to identify the batteries, e.g., aqueous/non-aqueous, low/high power and according to their size.

Primary batteries, which are also called non-rechargeable batteries, utilize the chemicals only once. After the first discharge, they are discarded. Having good shelf life, high energy density at low to moderate discharge rate, mostly small and ease of use are the general advantages of primary batteries. In addition to the mentioned advantages, they are also cheap and light, which makes them a convenient power source for portable electric and electronic devices [6].

Secondary batteries, which are also called rechargeable batteries, can be recharged electrically after discharge rather than being discarded. While recharging, the current is passed through the opposite direction of the discharge current. Since

electrical energy is stored, it is also known as “storage batteries” or “accumulators” [5].

In terms of usage of secondary batteries, it is classified under two subgroups. The first application is to use it as an energy storage device. There is a need for a primary energy source for charging and the device is mostly connected to this source. When there is demand, energy is delivered. These types of secondary batteries are used in automotive and aircraft systems. The second application is to use it as a primary battery while discharging and but can be recharged after usage rather than replaced. This type of secondary battery is used in portable consumer electronics, power tools, electric vehicles etc. Having high power density, flat discharge curve, and good low-temperature performance are the properties of the secondary batteries in addition to their rechargeability [5].

Lithium-ion is the most popular rechargeable battery chemistry used today. Lithium-ion batteries power the devices we use every day, like our mobile phones and electric vehicles [7] They consist of an electrolyte separating the two electrodes from the cathode and anode. Lithium ions are removed from the cathode and transported to the anode, where they are stored, during charging. Lithium ions migrate from the anode to the cathode when the process is reversed during discharge, producing electricity. Compared to other battery types like lead-acid and nickel-cadmium (NiCad), LIBs provide several benefits. They can store more energy per unit of mass or volume because they have a higher energy density. Additionally, they can be charged and discharged more frequently without significantly degrading because they have a longer cycle life. To sum up, because LIBs do not contain hazardous heavy metals, they are more environmentally friendly than lead-acid batteries [1].

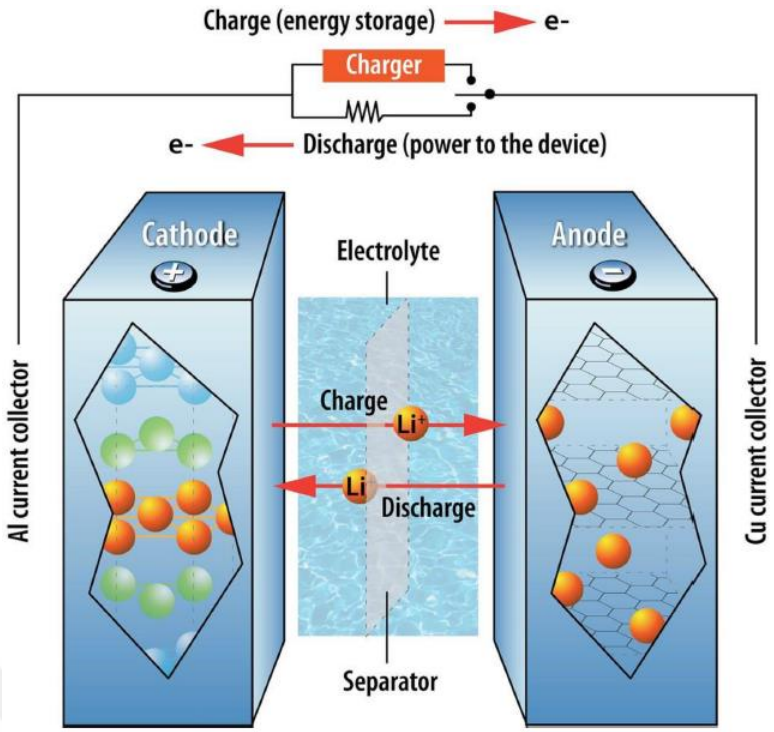

Figure 2.1: Schematic diagram of LIB [2].

2.1.2 Anode materials of lithium-ion batteries

In a lithium-ion battery, the anode is the electrode that accepts electrons during discharge, releasing lithium ions that go through the electrolyte to the cathode. Lithium ions are delivered to the anode during the charging process, which turns around the discharge process by releasing electrons. The performance, price, and safety of a lithium-ion battery are significantly influenced by the anode material. As a result, various anode material types have been researched and created to enhance lithium-ion battery performance.

2.1.2.1 Graphite

Due to its high specific capacity, low cost, and outstanding cycling stability, graphite is the most often utilized anode material in commercial lithium-ion batteries. A graphite-lithium intercalation compound (GLC) with a theoretical capacity of 372 mAh/g can be created when lithium ions are reversibly intercalated between the layers of graphite. However, due to several factors, such as the formation of the solid electrolyte interphase (SEI), irreversible capacity loss (ICL), and lithium plating, the practical specific capacity of graphite anodes is typically lower than the theoretical capacity [8].

During the first few cycles, the graphite anode develops a layer called the SEI that helps the battery's cycling stability by stopping further electrolyte decomposition. However, some lithium ions are irreversibly consumed by the SEI formation, decreasing the anode's useful capacity. The production of new phases that irreversibly consume lithium ions or the irreversible formation of surface films are both causes of the ICL, which is another reason for the capacity reduction in graphite anodes. Lithium plating, which can result in the deposition of metallic lithium on the anode surface and lower the cycle stability and safety of the battery, can happen at low temperatures or rapid charging rates [2].

The use of nanoscale graphite particles, surface coating with conductive polymers or carbon materials, and the addition of silicon or other alloying materials to increase the specific capacity and lessen the SEI and ICL effects are a few modifications that have been suggested for graphite anodes to get around these restrictions [2].

2.1.2.2 Silicon and silicon based materials

Due to their high theoretical specific capacity (up to 4200 mAh/g), low voltage hysteresis, and abundance in nature, silicon and silicon-based materials, such as silicon oxide, silicon carbide, and silicon-graphene composites, have drawn a lot of interest as potential anode materials for lithium-ion batteries. A lithium-silicon (Li-Si) combination, which can store up to four times more lithium ions than graphite, can be created by alloying silicon with lithium [2].

However, during the lithiation and delithiation processes, silicon anodes experience significant volume expansion and contraction. This causes mechanical stress, pulverization, and loss of electrical contact, which can result in battery deterioration and failure. The use of porous or nanostructured silicon particles, the addition of carbon or metal coatings to improve the mechanical strength and conductivity, and the development of silicon-based composites with other materials, such as carbon, metal oxides, or polymers, to improve stability and electrochemical performance are just a few of the various approaches that have been suggested to address this problem [2].

2.1.2.3 Comparison of anode materials

The main characteristics, benefits, and drawbacks of several anode materials for lithium-ion batteries are summarized in Table 2.1. Graphite anodes, as indicated in the table, offer the benefits of being inexpensive, having a high specific capacity, and having good cycling stability, but they are constrained by irreversible capacity loss and lithium plating. Although silicon anodes can provide greater specific capacities than graphite anodes, they must contend with mechanical instability and deterioration. Other materials need to be developed and optimized despite having special qualities and potential [2].

Table 2.1: Comparison of anode materials [2].

Anode Material	Theoretical Capacity (mAh/g)	Advantages	Disadvantages
Graphite	372	Low cost, high specific capacity, good cycling stability	Irreversible capacity loss, lithium plating
Silicon	4200	High specific capacity, low voltage hysteresis	Mechanical degradation, instability

2.1.3 Cathode materials of lithium-ion batteries

One of a lithium-ion battery's most important parts, the cathode determines the battery's voltage, capacity, and overall performance. A cathode typically consists of a host material and a chemical that contains lithium to allow for the insertion and extraction of lithium ions during charge and discharge cycles. Metal oxides, such as lithium cobalt oxide (LCO), lithium nickel manganese cobalt oxide (NMC), lithium manganese oxide (LMO), and lithium iron phosphate (LFP), are the most popular cathode materials used in lithium-ion batteries. Each material has distinct qualities that make it appropriate for a variety of applications [1].

2.1.3.1 Lithium cobalt oxide (LCO)

Due to its high specific capacity and good cycling stability, LCO is a commonly used cathode material for high-energy-density applications, such as EVs and consumer electronics. LCO has 130-150 mAh/g specific capacity. LCO does have certain disadvantages, though, including a high price, a little supply, and safety issues connected to its instability at high temperatures [9].

2.1.3.2 Lithium manganese oxide (LMO)

LMO is a cathode material that is suitable for power tools, e-bikes, and other high-power applications due to its strong thermal stability and good cycling stability. It has between 90-130 mAh/g specific capacity. Comparatively speaking to other cathode materials, LMO is also rather inexpensive. However, compared to other cathode materials, LMO has a lower specific capacity and energy density, which restricts its suitability for high-energy-density applications [9].

2.1.3.3 Lithium nickel mananese cobalt oxide (NMC)

Another high-energy-density cathode material frequently utilized in EVs is NMC. It features a 150-180 mAh/g specific capacity. Compared to LCO, NMC has a number of benefits, including cheaper costs and improved thermal stability. The reduced cycling stability and increased vulnerability to oxygen release during cycling, which can result in thermal runaway and safety concerns, are two downsides of NMC [9].

2.1.3.4 Lithium iron phosphate (LFP)

In stationary storage and low-power applications, such as power tools and e-bikes, LFP is a cathode material with outstanding safety, a long cycle life, and a low cost. It features 160-180 mAh/g theoretical capacity. About other cathode materials, LFP has a number of benefits, including superior thermal stability, low toxicity and lower susceptibility to oxygen release during cycling. LFP's usefulness for high-energy density applications is constrained by the fact that it has a lower energy density than other cathode materials [9].

2.1.3.5 Comparison of cathode materials

A common cathode material is $LiCoO_2$ (LCO), which has a high specific capacity and energy density. It is less acceptable for several applications due to its weak thermal stability and safety issues. A less expensive option, $LiMn_2O_4$ (LMO), has a lower energy density but strong thermal stability and cycling stability. Another well-liked cathode material is $LiFePO_4$ (LFP), which has good thermal stability and safety but a lower specific capacity and energy density. NMC ($LiNiMnCoO_2$), a cathode material with a high specific capacity, good thermal stability, and cycling

stability, combines the benefits of both LCO and LMO [9]. They are summarized in Table 2.2.

Table 2.2: Comparison of cathode materials [6]

Cathode Material	Nominal Voltage (V)	Specific Capacity (mAh/g)	Cost	Thermal Stability	Cycling Stability	Safety
LCO	3.7	130-150	High	Poor	Good	Safety concerns at high temperatures
LMO	4.0	90-130	Low	Good	Good	Moderate
NMC	3.7-4.3	150-180	Medium	Good	Good	Moderate
LFP	3.3	160-180	Low	Excellent	Excellent	Excellent

2.1.4 Electrolyte

During charge and discharge cycles, the electrolyte acts as a channel for ionic conduction between the cathode and anode, permitting the passage of lithium ions. A lithium-ion electrolyte that meets all the criteria is optimal. High ionic conductivity is essential for enabling effective ion movement throughout the battery. This quality is essential for decreasing internal resistance and producing high power output. A suitable electrochemical stability window must also be present in the electrolyte for safe operation within the specified voltage range. The properties of the electrolyte are significantly influenced by its composition. Due to their generally high dielectric constants and low viscosities, common solvents like ethylene carbonate (EC) and dimethyl carbonate (DMC) provide an ideal environment for ion transport. Lithium salts that dissociate into lithium ions and anions, such as lithium hexafluorophosphate (LiPF6) and lithium hexafluoroarsenate (LiAsF6), are added to increase conductivity. Additives are frequently used to improve electrolyte function even more. In addition to enhancing conductivity and stabilizing the electrolyte, these chemicals also generate protective layers on the electrode surfaces. They can improve battery efficiency and reduce adverse effects that cause electrolyte breakdown [10].

Despite this, there are still issues with lithium-ion electrolytes. Capacity loss, a shorter cycle time, and safety risks might result from electrolyte breakdown and side reactions. Researchers are actively looking for ways to reduce these problems and increase electrolyte stability. To address the demands of cutting-edge cathode

materials that function at high potentials, high-voltage electrolytes are also being developed [10].

Solid-state electrolytes have become a possible replacement for liquid electrolytes in recent years. These primarily inorganic or polymer-based substances provide higher levels of stability, compatibility, and safety with high-energy electrode materials. Future developments in lithium-ion battery technology could greatly benefit from the intensive research being done on solid-state electrolytes [10].

Ions can efficiently flow between the cathode and the anode thanks to the electrolyte, which is a crucial component of lithium-ion batteries. Research & development activities continue to be driven by the search for electrolyte materials with high conductivity, stability, and compatibility, with the goal of enhancing battery performance, safety, and reliability for a variety of applications [10].

2.1.5 Separator

Between the cathode and the anode, the separator serves as a physical barrier that prevents physical contact and short circuits between the two electrodes while enabling lithium ions to pass through. A lithium-ion separator's main function is to make it easier for ions to move while yet maintaining electrical insulation. To ensure the battery operates safely and effectively, it must have a number of essential qualities. To allow the passage of lithium ions over its surface, the separator must first have strong ionic conductivity. This attribute has a direct impact on the battery's overall performance and power output. Separators must also be mechanically strong and stable in order to survive the internal stresses and strains brought on by battery cycling and handling. To prevente electrode deformation and maintain efficient ion transport channels, the separator must keep its structural integrity. Meeting these parameters requires careful consideration while choosing separating materials. Polypropylene (PP), polyethylene (PE), and ceramic-coated separators are three frequently utilized separator materials. Excellent flexibility, strong thermal stability, and great mechanical strength are all features of PE and PP separators. Aluminum oxide (Al_2O_3) or polymeric ceramic coatings are used to improve the separator's thermal stability and safety, especially in high-temperature and abusive situations. The performance and safety of batteries are continually being improved by investigating new separator designs and technologies. For instance, composite separators with higher mechanical

and thermal stability are now being developed. To further increase battery performance and longevity, functionalized separators with attributes including improved wettability and improved electrode-separator interface interactions are being researched [11].

In conclusion, it should be noted that lithium-ion separators are essential to the safe and dependable operation of lithium-ion batteries. These separators offer effective ionic conduction between the cathode and anode in addition to electrical isolation. Separator material and design improvements continue to enhance battery performance, safety, and overall viability in a variety of applications [11].

2.2 Ageing Mechanism of Lithium-Ion Batteries

2.2.1 General overview

Due to their high energy density and long cycle life, lithium-ion batteries are frequently employed in portable electronic gadgets, electric cars, and fixed energy storage systems. However, with the rise in demand for high-performance batteries, lithium-ion battery ageing has turned into a serious problem. Lithium-ion batteries age as a result of a progressive decline in performance over time, which reduces the amount of time they may be used. Lithium-ion battery ageing is a multi-step process that includes a number of variables, such as chemical reactions, structural alterations, and temperature effects [12].

2.2.2 Reasons for ageing

Due to the ageing processes that take place when lithium-ion batteries are used, their lifespan is constrained. Developing ways to increase the lifespan of batteries requires a thorough understanding of the causes of ageing. An overview of the main causes of lithium-ion battery ageing will be given in this chapter.

2.2.2.1 Side reactions

Inadequate working conditions, like excessive temperatures or overcharging, cause side reactions in lithium-ion batteries. The anode or cathode may develop a solid-electrolyte interface (SEI) layer as a result of side reactions, which may result in a reduction in capacity and an increase in resistance. Electrolyte breakdown and interaction with the electrode surface result in the formation of the SEI layer.

Therefore, the development of an SEI layer is an irreversible process that over time may result in a significant decline in battery performance [13].

2.2.2.2 Cycling

Another factor contributing to lithium-ion battery ageing is cycling. The volume of the electrode's active material changes with each cycle of charging and discharging, which may cause mechanical strains in the electrode's structure. The electrode may crack or delaminate as a result of these forces, losing its active material and decreasing its capacity. A SEI layer may also develop on the anode or cathode as a result of repetitive cycling, as was already noted [3].

2.2.2.3 Storage conditions

A lithium-ion battery's lifespan may be impacted by how it is stored. The battery experiences self-discharge when kept at high temperatures, which may result in the creation of an SEI layer on the anode or cathode. When the battery is later used, the creation of an SEI layer can significantly lower battery performance. Additionally, keeping the battery at a low state of charge might speed up ageing because doing so can result in lithium plating on the anode, which lowers capacity and raises safety issues [3].

2.2.2.4 Contamination

Lithium-ion battery ageing can also be caused by contamination. The electrolyte can react with contaminants like moisture, oxygen, and other gases to degrade the performance of the battery. As discussed earlier, contamination can also result in the development of an SEI layer on the anode or cathode. In order to prevent contamination, it is crucial to make sure that the battery is created and stored in a clean and controlled environment [3].

2.2.3 Effects of ageing on lithium-ion batteries

Ageing is an inevitable process that happens over time to lithium-ion batteries. The performance, safety, and general longevity of the battery may be adversely affected by a number of problems that may result from this approach. We will discuss the various consequences of lithium-ion battery ageing in this chapter.

2.2.3.1 Capacity fade

Capacity fading is one of the most important impacts of lithium-ion battery ageing. Capacity fade is the gradual loss of the battery's ability to hold a charge, which lowers the battery's overall capacity. The driving range and general performance of electric vehicles, which rely on lithium-ion batteries for power, may suffer as a result of this loss in capacity. Several ageing factors, including cycling and side reactions, which result in a loss of active lithium ions in the battery, cause capacity fading. The battery's capacity is decreased as a result of the loss of active lithium ions, and it can no longer store as much energy as it could when it was brand-new [14].

2.2.3.2 Increase in internal resistance

The internal resistance of a lithium-ion battery rises with time. Internal resistance is the resistance to current flow within the battery that causes a voltage drop across the battery terminals. The battery's total energy efficiency decreases when internal resistance rises because more energy is lost inside the battery. The battery's power output may also drop as a result of an increase in internal resistance because it won't be able to supply the load with as much current as it could have when it was new. This may result in a decrease in battery performance, especially for applications requiring high power output, such as electric automobiles [14].

2.2.3.3 Safety issues

Lithium-ion battery ageing can potentially cause safety problems, especially if the battery is overcharged or is exposed to extreme heat. The solid electrolyte interface (SEI) layer that forms on the anode or cathode as a battery ages decreases the battery's capacity to store or discharge energy. The SEI layer may fail in a battery that has been overcharged or exposed to extreme heat. This quick energy release may result in thermal runaway and an uncontrolled rise in internal battery temperature. This makes it crucial to keep an eye on the battery's temperature both while charging and using because it could cause a fire or explosion [14].

2.2.3.4 Decreased lifespan

Finally, aging in lithium-ion batteries can result in a reduction in the battery's overall lifespan. Due to the accumulation of deterioration mechanisms over time, including capacity fading, an increase in internal resistance, and safety concerns,

lifespan is decreasing. Although lithium-ion batteries are made to endure for many years, the aging process can drastically reduce their lifespan. This could result in a decline in the battery's overall performance and dependability, necessitating the creation of techniques for extending the life of lithium-ion batteries. The performance, safety, and total longevity of the battery can all be adversely affected by ageing in lithium-ion batteries due to a variety of causes. Among the most important effects of aging are capacity decline, a rise in internal resistance, safety concerns, and a reduction in lifetime. Therefore, it is essential to comprehend ageing mechanisms and create mitigation techniques in order to create secure and dependable lithium-ion batteries [14].

2.2.4 Prevention methods of ageing in lithium-ion batteries

Lithium-ion battery aging is a major issue for the business since it affects the battery's capacity, performance, safety, and lifespan. However, there are a number of ways to stop or delay the aging of lithium-ion batteries. We'll discuss some of the most cutting-edge and successful strategies for preventing lithium-ion battery ageing in this chapter.

2.2.4.1 Cell design

Another important factor in delaying ageing is the design of the electrodes in lithium-ion batteries. The ageing mechanisms in the battery can be impacted by the material selection and electrode structure. For instance, utilizing high-capacity electrodes can boost the battery's capacity, but it can also hasten ageing owing to adverse effects. Therefore, creating electrodes that reduce degradation mechanisms can aid in extending the battery's life. This can be accomplished by utilizing materials that are resistant to adverse reactions, enhancing the composition of the electrolyte, and creating electrodes that are less stressful during cycling [14].

One of the most promising solutions for reducing the effects of ageing in lithium-ion batteries is silicon anodes. Theoretically, silicon has a large capacity, which could boost the battery's energy density. Considerable volume changes experienced by silicon anodes during cycling, on the other hand, cause mechanical deterioration and a loss of electrical contact between the anode and the electrolyte. Numerous strategies have been devised to address this problem, including the usage of silicon with nanostructures, silicon-carbon composites, and other cutting-edge

materials. These techniques can reduce the impact of volume variations and increase the silicon anode's overall stability, extending the battery's lifespan and enhancing performance [2].

Another cutting-edge technology that helps lithium-ion batteries age more slowly is solid-state electrolytes. Higher energy density, better safety, and greater stability than liquid electrolytes are just a few advantages that solid-state electrolytes can offer. By minimizing the creation of the SEI layer, which over time can reduce the battery's performance, solid-state electrolytes can help lessen the impacts of ageing. Additionally, solid-state electrolytes can stop active materials from dissolving, lowering the loss of active lithium ions and enhancing the battery's total capacity and lifespan [10].

2.2.4.2 Advanced control systems

Additionally, modern control systems can lessen the effects of lithium-ion battery ageing. A battery's temperature, voltage, and other characteristics can be monitored by sophisticated control systems, enabling real-time optimization of the battery's performance and life. The risk of thermal runaway and other safety hazards can be decreased by these systems' ability to prevent overcharging and overheating.

One of the best ways to stop lithium-ion batteries from ageing is thermal control. High temperatures hasten the battery's ageing process, which reduces capacity, performance, and safety. As a result, maintaining the battery's temperature during charging and discharging is essential for maximizing lithium-ion battery life. Thermal buffering, active cooling, and passive cooling are a few examples of thermal management strategies that can be applied. Active cooling involves employing a cooling system to remove heat from the battery pack, whereas passive cooling entails engineering the battery pack to dissipate heat naturally. The use of a substance that can absorb or release heat is known as thermal buffering, and it is used to keep the battery pack's temperature stable [13].

Managing the state of charge (SOC) in lithium-ion batteries is another efficient way to stop them from ageing. To prevent overcharging or over discharging the battery, SOC management entails regulating the amount of charge that the battery can store. A battery's capacity may be decreased and its internal resistance may rise as a result of overcharging or over discharging the battery, which may also result in the

production of a solid electrolyte interface (SEI) layer. Therefore, maintaining the battery's SOC throughout charging and draining is essential for maximizing battery life. A battery management system, which keeps an eye on the battery's voltage, current, and temperature to make sure it functions within safe bounds, can help with this [13].

Equalizing the voltage and capacity of individual cells inside a battery pack is the process of balancing. Individual lithium-ion battery cells' capacities and voltages can shift over time, reducing performance and posing safety risks. Therefore, putting in place a good balancing mechanism might help to keep the battery from deteriorating. Improved performance and increased longevity can result from keeping the cells in a pack at a constant voltage and capacity level using a balancing system. Maintaining a balanced state, can be done by using passive or active balancing techniques that can transfer charge between cells [13].

2.3 Thermal Runaway Mechanism of Lithium-ion Batteries

Due to their high energy density, low self-discharge rate, and long cycle life, lithium-ion batteries have emerged as the preferred option for many applications. However, they are not impervious to failure, and when they do, it may result in disastrous events like fires and explosions. Thermal runaway is one of the most frequent ways for lithium-ion batteries to fail. The battery experiences thermal runaway, a self-sustaining reaction that causes a rapid rise in temperature, gas evolution, and energy release. The thermal runaway is thought to have been caused by oxygen species that the cathode has liberated. The electrolyte in the area has a significant impact on the thermally driven oxygen species release route. The thermal stability of the cathode is adversely affected by the electrolyte, which may promote phase change and oxygen release. Thermal runaway is caused by the reactivity of oxygen species with the electrolyte [15] .

2.3.1 Trigger methods

In this chapter, it will be discussed the different triggering methods that can lead to thermal runaway in lithium-ion batteries.

2.3.1.1 Internal short circuit

When a conducting substance like metal fragments, dendrites, or a separator breaks down inside the cell and creates a direct connection between the anode and cathode, it might result in an internal short circuit. Due to the high current flow and localized heating that results, thermal runaway may occur. Manufacturing flaws, electrode contamination, or mechanical damage sustained during handling and use can all result in internal short circuits [16].

2.3.1.2 External heating

External heating may result via contact with a heat source, exposure to high ambient temperatures, or a breakdown in thermal insulation. The battery may become thermally runaway due to external heating, which will trigger an accelerated chain of events. In situations where the battery is exposed to high temperatures, such as in electric vehicles, where the battery may be exposed to high ambient temperatures or near hot components, this can be particularly problematic [16].

2.3.1.3 Overcharging

When a battery is charged above the safe working voltage range, this is known as overcharging, and it causes metallic lithium to precipitate on the anode surface. A solid electrolyte interphase (SEI) layer may form as a result of the deposited lithium causing a decrease in the electrolyte decomposition voltage. However, if the overcharging persists, it may cause the SEI layer to fail, resulting in the creation of lithium metal and thermal runaway. This layer can stop future lithium deposition [16].

2.3.1.4 External mechanical damage

Internal short circuits and thermal runaway can result from physical damage to the battery cell caused by external mechanical damage such as puncture, compression, or bending. This may happen as a result of careless handling or mishaps while being transported, stored, or used [16].

2.3.2 Energy release mechanism of thermal runaway

Lithium-ion batteries that experience thermal runaway may experience an uncontrollable rise in temperature and pressure that results in the release of a sizable

quantity of energy. Heat creation, thermal propagation, and energy release are the three phases of the mechanism that releases energy during thermal runaway.

2.3.2.1 Heat generation

The first temperature rise that starts the thermal runaway process is a part of the heat generating stage. Numerous things, such as an extremely hot environment, an overcharged battery, or physical damage to the battery, might cause this. Exothermic processes inside the battery cause heat to be produced at a faster rate when the battery's temperature rises [16].

2.3.2.2 Thermal propagation

The thermal runaway process can quickly spread throughout the battery after the heat generating stage has begun, which causes a further rise in temperature and the release of more energy. Internal short circuits, separator overheating, or thermal runaway in an adjacent cell are just a few causes of thermal propagation that might happen. Thermal breakdown processes can start within the electrolyte and electrodes during thermal propagation, when the battery's temperature might rise quickly. This could result in the emission of combustible gases like hydrogen and methane, which could further raise the battery's internal pressure and help the thermal runaway process spread [16].

2.3.2.3 Energy release

Significant amounts of energy are released in the form of heat and gas during the latter step of the thermal runaway energy release mechanism. The breakdown of the battery's active components causes gas evolution, which can result in the release of hazardous and combustible gases such as carbon monoxide, carbon dioxide, and hydrogen. A fire or explosion may arise from the expelled gases igniting, which can cause flame propagation. Rapid internal component expansion of the battery can cause mechanical deformation, which might result in ruptures or deformations [16].

Thermal runaway can result in a massive energy release that has the potential to endanger nearby people as well as damage nearby equipment. The battery's size and capacity, the degree of thermal runaway, the kind of electrolyte and electrodes used in the battery, and other variables all affect how much energy is released.

2.3.3 Safety strategies

Lithium-ion battery thermal runaway can result in disastrous outcomes like fires, explosions, and hazardous gas releases. Therefore, it is crucial to put safety measures in place that can stop, lessen, or regulate thermal runaway.

2.3.3.1 Cell design and materials selection

Designing battery cells with safety features that can stop or lessen thermal runaway is one of the main safety measures. For example, employing lithium iron phosphate cathodes, which have a lower risk of thermal runaway than alternative cathode materials like lithium cobalt oxide, which is more prone to thermal runaway. To avoid or lessen thermal runaway, safety elements including shut-off mechanisms, pressure relief valves, and separators can be incorporated into the cell design. For instance, the electrodes in certain batteries are connected by a ceramic separator that melts at high temperatures, stopping further thermal runaway. The separator's design may also incorporate elements that can endure high temperatures, such as enhanced porosity, thickness, and the usage of ceramic or polymer materials. These characteristics can improve battery thermal stability and short circuit protection, enhancing safety [17].

2.3.3.2 Thermal management

To prevent and manage thermal runaway in lithium-ion batteries, effective thermal management is essential. The danger of thermal runaway can be reduced by managing the battery's temperature. This can be done by employing heating or cooling techniques such as phase change materials, passive air cooling, or liquid cooling. By including high thermal conductivity materials into the design of the cell or by giving the cells particular structural features that facilitate effective heat transfer, thermal management can also be incorporated into the cell design [17]. Furthermore, Wencan, and others states that good thermal system and enough heat dissapation could increase the thermal propagation performance [18].

2.3.3.3 Protection systems

To monitor and manage the battery's condition, a battery management system is necessary. This involves keeping an eye on the battery's temperature, charge level, and overall health. The BMS can avoid or mitigate thermal runaway by monitoring

these parameters, managing the battery's charging and discharging, and notifying the user or system in case of abnormal situations. To avoid or reduce thermal runaway, the BMS might also have safety features like overcurrent protection, overvoltage protection, and undervoltage protection. Additionally, the BMS can regulate cell balancing to avoid thermal runaway caused by individual cells being overcharged or over discharged. The system can also include crush sensors, pressure sensors, and gas sensors to improve the BMS detection algorithm [17].

To prevent overcharging, over discharging, and short circuits, a battery can be protected using passive safety devices like fuses and circuit breakers. The chance of thermal runaway can be decreased by avoiding these occurrences.

2.3.3.4 Battery packaging

Thermal runaway can be avoided in part by the battery's packaging. The packaging should be made to stop external influences from harming the battery and causing thermal runaway, such as mechanical stress or punctures.

The packaging may have elements like strengthened casings, insulation, and shielding coatings that can assist shield the battery from mechanical harm and increase its thermal stability. Using foams between the cells may have a great impact improving thermal propagation performance. For instance, it is stated in “An Experimental Study on Preventing Thermal Runaway Propagation in Lithium-Ion Battery Module Using Aerogel and Liquid Cooling Plate Together” using aerogels which is basically foams that have low thermal conductivity between the cells improved the thermal propagation performance dramatically [19]. Additionally, Lvwei and others states the importance of casing of the lithium-ion cells by comparing thermal runaway performance of pouch and prismatic cells [20].

In the event of a thermal runaway incident, it is crucial to control and lessen its impacts. This involves making the battery pack enclosure out of flame-resistant materials and giving it enough ventilation to get rid of heat and harmful fumes.

Designing the battery pack with numerous compartments is another containment strategy that can be used to stop thermal runaway from spreading to adjacent cells. To immediately put out any potential fires, automatic fire suppression devices like sprinklers or fire extinguishers can also be installed.

Several variables, including the application, battery chemistry, and operating conditions, can affect how effective thermal runaway safety measures are in lithium-ion batteries. In order to achieve the best level of safety, it is often advised to combine many safety techniques. In the absence of external triggers like mechanical abuse or short circuits, cell design and material selection may not be sufficient to stop thermal runaway from happening in the first place. Although thermal runaway may not always be completely avoided, thermal management and BMS can help to lessen its impacts. In the event of a thermal runaway incident, containment and ventilation are crucial to limiting damage and guaranteeing the safety of the immediate area.

In conclusion, thermal runaway is a serious safety risk for lithium-ion batteries, and it is critical to comprehend its causes, energy release mechanisms, and safety precautions in order to avoid disastrous outcomes like fires and explosions.

3. EXPERIMENTAL STUDIES

The objective of this study is to select the optimum foam material for EV HV battery pack modules and optimize the thermal propagation duration at the battery pack level. Silicon-based foams were placed between cells inside the modules. Figure 3.1 shows the structure of the modules and the location of the foams. First, two tests were conducted to determine the thermal runaway trigger method. Subsequently, three mini module level tests were performed with using three different foams to extract the thermal propagation durations from cell to cell. The foams were evaluated in terms of their thermal conductivity, compression force, and thermal propagation duration. Finally, three-pack level tests were performed to determine the optimal thermal propagation time.

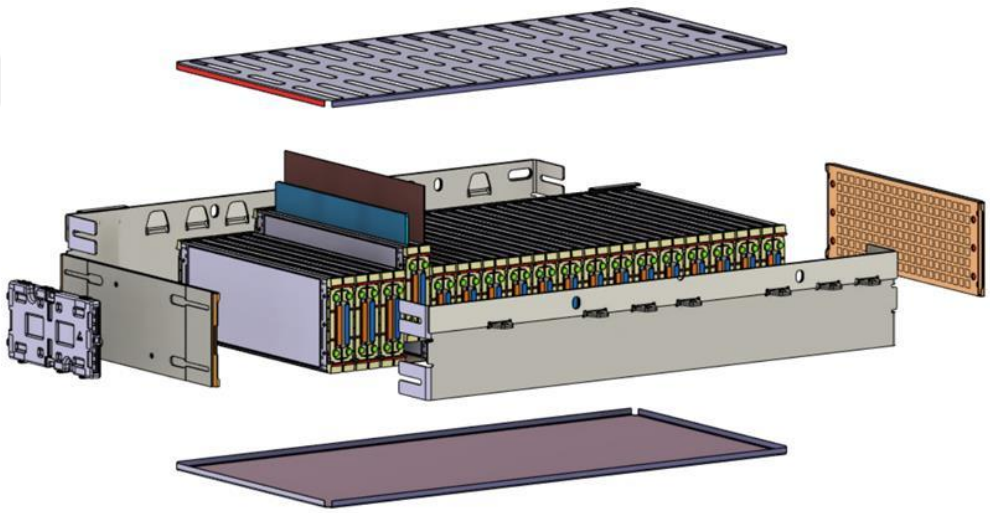

Figure 3.1: Module schematic

G/NMC 73 Ah pouch lithium-ion cells were used as test objects. The detailed specifications of the cell can be found below in Table 3.1.

Table 3.1: Cell specifications

Item	Value
Chemistry	G/NMC
Type	Pouch
Weight [g]	930
Dimensions [mm]	101x364x14.2
Nominal capacity [Ah]	73
Nominal voltage [V]	3.65
Maximum voltage [V]	4.20
Specific energy [Wh/kg]	291
Energy [Wh]	271
Peak discharge current @ 25° 10s [A]	650A
Continuous discharge current @ 25° [A]	220A
Continuous charge current @ 25° [A]	36.5A

3.1 Comparison of Trigger Methods

In a study that was made by Xin, Shuyu, Huaibin, Yuejiu, Xuning, triggering methods heating, nail piercing, and overcharging was compared. First, TR was induced on a modified cell using one of the three triggering modes. The TR and TP models were then developed for each trigger mode, and the model parameters were determined by experimentation. Third, the three triggering modes' effects on the battery module TP properties were examined. Finally, during the TP, the energy flow distribution was determined. The following were the primary conclusions: (1) In the early stage of TP, the differences in TP time and triggering temperature are evident under various trigger mechanisms, but these disparities gradually disappear in the later stage of TP. As a result, choosing a TR trigger mode is crucial during the first phase of TP. The heated trigger offers the best overall performance while the nail penetration trigger has the quickest trigger time, enabling good LIB testing operability and resulting in minimal costs. (2) The energy flow distribution reveals that more than 26% of TR energy is released during cell material explosions and more than 60% of TR energy is used for battery self-heating [20].

In this study, overcharge and external heating methods were considered after reviewing the leiterature, standard which is UL 9450A and regulations which are UN ECE R100 revison 3 and UN GTR 20 [22,23,24]. Additionally, tests on the module level were executed to find the best triggering method. Since the nail penetration method is uncontrollable and opens an unwanted venting hole, it was considered that the method is not worth testing.

3.1.1 Overcharge triggering method

3.1.1.1 Test object

A 6S3P module was used as the test object. In this configuration, three cells were connected in parallel and parallel groups were connected in series. The foams were placed near each cell. The cell stack was covered with an aluminum housing. Cables were extracted from the cell 1 terminals through the housing to the outside to execute overcharging. The thermocouples were located inside the module in the middle of the cell surfaces. The structure and thermocouple locations are shown in Figure 3.2. The module was charged to 100% SOC, which was approximately 25 V before the test was started.

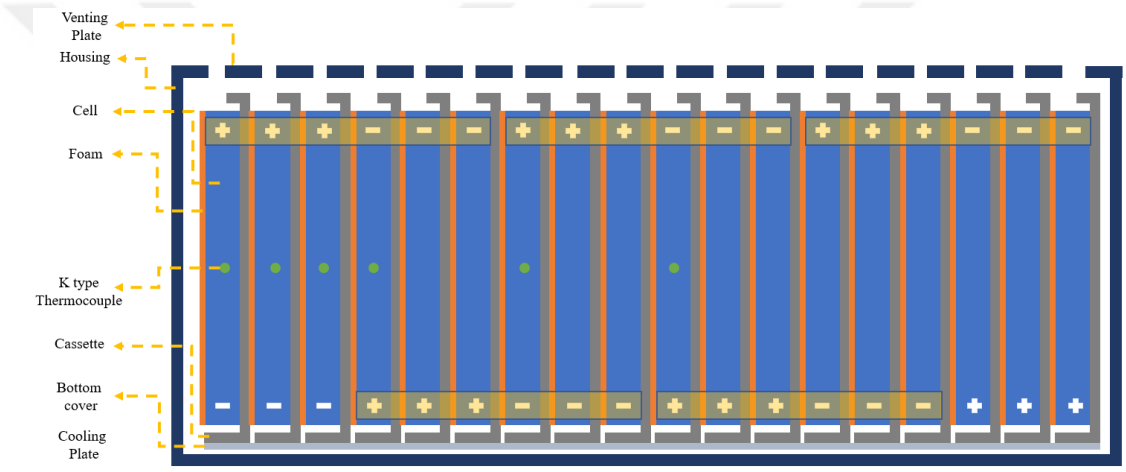

Figure 3.2: Test object sketch for overcharge triggering method

3.1.1.2 Test details

The test object was placed in a safe environment. All measurement data were logged via datalogger using CAN Bus communication. Vector 1640A was used to connect the data logger to a computer. Data were observed using Vector CANoe on a test laptop. The first cell was started to be charged with 25 A and after around 53 minutes thermal runaway incident was observed. Thermal propagation continued until all cells were burnt. Figure 3.3 shows trigger cell voltage and temperature. As can be seen, once the TR started, the voltage of cell 1 started to decrease, and then the voltage measurement point short-circuited to the neighboring cell, therefore, it started to show module voltage which is nearly 18 V. At the same time with the voltage drop, cell temperature suddenly increased over 600 °C and then started to decrease since the energy inside the cell was released due to thermal runaway.

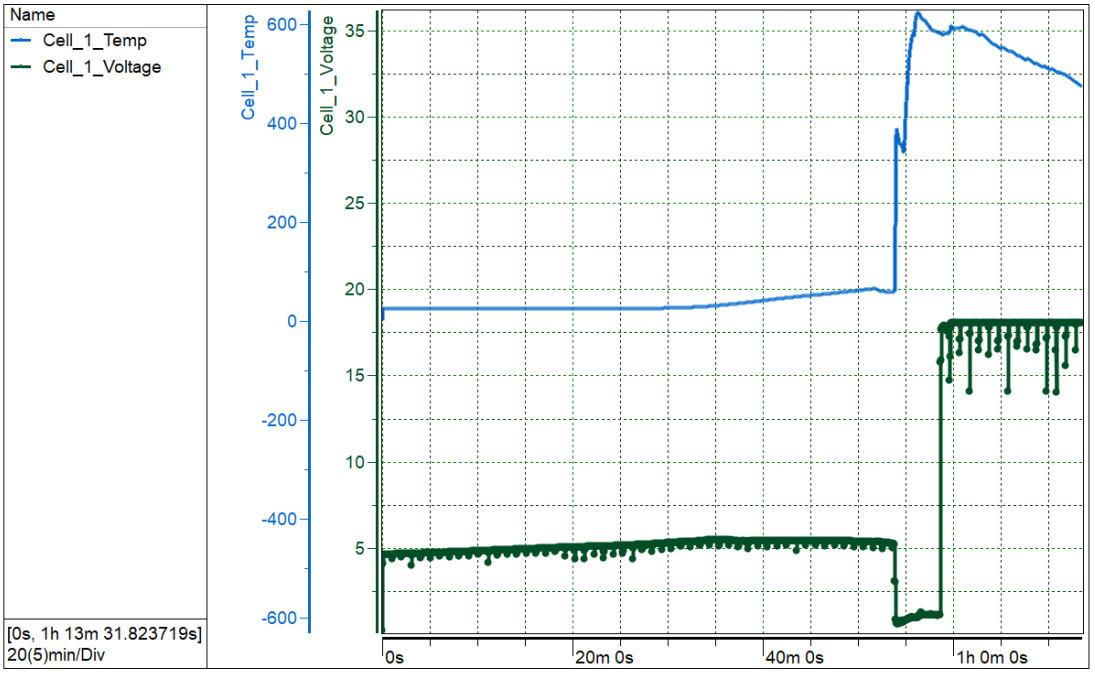

Figure 3.3: Trigger cell temperature and voltage graph

3.1.2 Heating triggering method

3.1.2.1 Test object

Similar to the overcharge-triggering test, the object was a 6S3P module. In this configuration, three cells were connected in parallel and parallel groups were connected in series. The foams were placed between the cells. The cell stack was covered with an aluminum housing. 300 W heating pad was used and placed in the middle of the cell 1 surface to provide external heating. Thermocouples were located in the middle of the cell surfaces and the heating pad. Voltage measurement cables were connected to the positive and negative terminals of the module. The structure and thermocouple locations are shown in Figure 3.4.

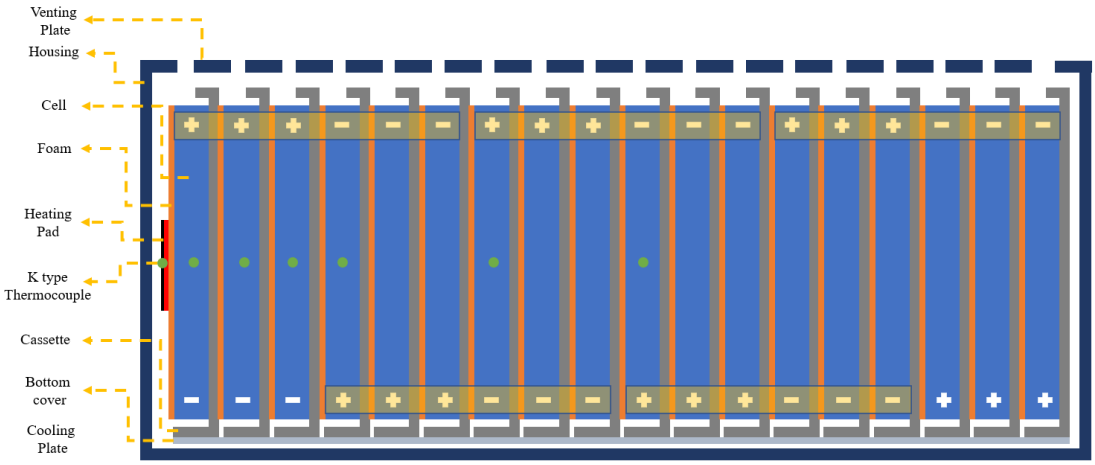

Figure 3.4: Test object sketch for heating triggering method

3.1.2.2 Test details

The test object was placed in a safe environment. Thermocouples and voltage measurement cables were plugged into a datalogger, through the datalogger data were observed and logged via a test laptop. At the beginning of the test, the heating pad was powered with 220 V AC voltage to initiate a thermal runaway. The first cell started to be heated after around 45 seconds and thermal runaway immediately started. Once the TR was observed, the power of the heating pad was cut off. Thermal propagation continued until all cells were burnt. Figure 3.5 shows the trigger cell temperature and heating pad temperature. As can be seen in Figure 3.5, cell temperature increased to approximately 900 °C in seconds. The peak above 1200 °C in the graph just shows the momenteraly measurement error.

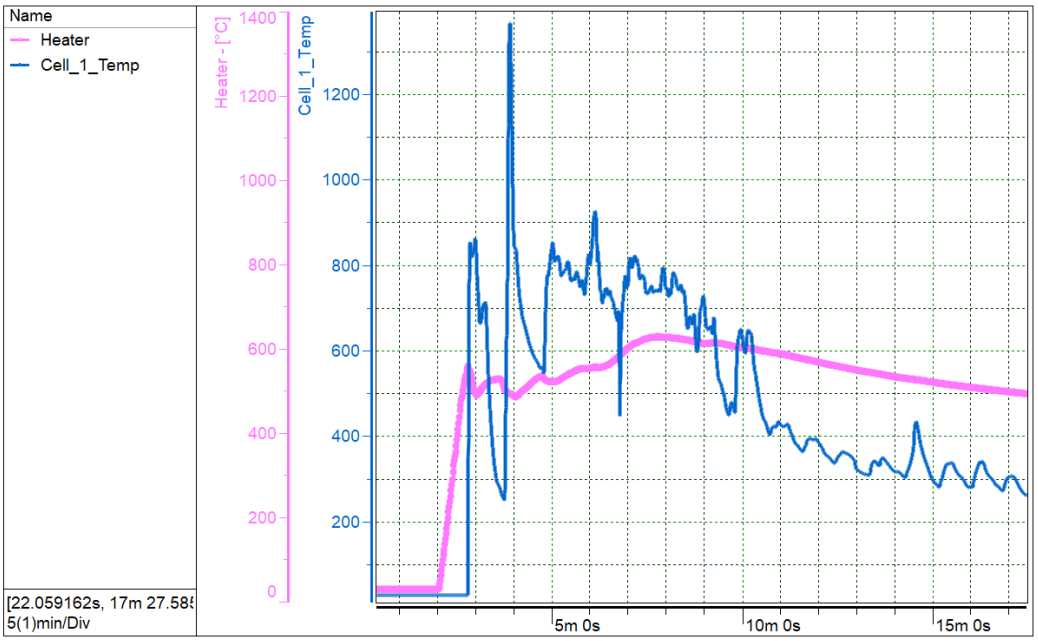

Figure 3.5: Trigger cell temperature and heating pad temperature

3.2 Comparison of Foams

Foam is frequently employed in the design of battery modules for high voltage lithium-ion pouch cells for several reasons. Since the foam is a good insulator, it can be used for thermal management in the battery. During operation, lithium-ion batteries can produce a lot of heat, which can lead to long-term degradation or even fire. By creating a barrier of insulation between the cells and their surroundings, foam can assist in controlling the battery's temperature. On the other hand, foam can also aid in giving the battery module mechanical stability. Due to their relative softness and flexibility, lithium-ion pouch cells are susceptible to deformation and even puncture if improperly supported. The mechanical loads, shocks and swelling that the battery could undergo while operating can be distributed using. Hence, the life cycle of cells would be extended. Finally, foam can also assist in providing electrical isolation between the battery module's cells. Due to their high reactivity, lithium-ion batteries have the potential to short circuit if they come into touch with one another. By establishing an insulating and non-conductive barrier between the cells, foam can aid in preventing this.

Overall, it is crucial for assuring the safety, dependability, and longevity of the battery to incorporate foam into the design of HV battery modules with lithium-ion

pouch cells. When constructing a battery module, it is essential to consider things like proper thermal management, mechanical stability, and electrical isolation. Foam can help with all these concerns.

In this study, three silicon based foams named X1, X2 and X3 were considered and compared. Due to the mechanical boundaries of the module, the thickness was selected as 2 mm before the study. They were flexible, compressible and ultra low density having 0.25- 0.40 g/cm^3. Additionally, the electrical isolation feature is adequate for all candidates.

In this chapter, foams will be evaluated in terms of their thermal conductivity, compression force displacement and thermal propagation impact.

3.2.1 Thermal conductivity impact

A material's capacity to conduct heat is determined by its thermal conductivity. The rate at which heat moves through a unit area of a material for every unit temperature change between two places is what is meant by this term. Watts per meter-kelvin (W/mK) or BTU per hour per foot-degree Fahrenheit (BTU/hr-ft-°F) are the two standard units used to measure thermal conductivity. Thermal conductivity refers to how quickly heat may pass through a material. High thermal conductivity materials are efficient heat conductors and can move heat quickly. Low thermal conductivity materials are poor heat conductors, which means they transfer heat slowly. For instance, metals with high thermal conductivity, such as copper and aluminum, are frequently employed as heat sinks in electronics. The low thermal conductivity of materials like wood and plastic, on the other hand, makes them effective insulators and a common choice for use in construction to stop the flow of heat [25].

Thermal conductivity is a crucial topic in the design of various devices, including batteries, where heat management is necessary for the greatest performance and safety. The composition, structure, and temperature of the material are some of the factors that affect thermal conductivity. The general tendency of materials to have high heat conductivity is influenced by factors such as high density, regular crystal structure, and strong chemical bonds. Thermal conductivity is influenced by temperature as well because it normally increases with a temperature differential between two places.

For batteries to operate effectively and safely, particularly in high-power and high-energy applications, thermal control is essential. High thermal conductivity batteries can disperse heat more effectively, lowering the chance of overheating and thermal runaway. Batteries frequently use materials like graphite, copper, and aluminum as heat conductive materials. However, in this design, cells are cooled from the bottom side, therefore, foams that are located on the surface of cells should have low thermal conductivity in order to slow down the heat distribution in case of thermal runaway of a single cell. Thermal conductivity values of the foams were given in Table 3.2.

Table 3.2: Thermal conductivity values

Product	Thickness [mm]	Thermal Conductivity <400°C [W/mk]	Thermal Conductivity >800°C [W/mk]
X1	2	0.09-0.10	0.17
X2	2	0.11-0.13	0.15
X3	2	0.04-0.06	0.10

3.2.2 Compression force displacement impact

The relationship between the compressive force and the associated displacement of material under compression is known as compression force displacement (CFD). In mechanical engineering, this relationship is crucial because it helps us comprehend how a material responds to compressive pressures and how it deforms in response to those loads. A material deforms and has a loss in height or volume when an external compressive force is applied to it. The displacement of the material can be used to calculate this deformation. The displacement changes as the applied compressive force rises, as shown by the compression force displacement relationship [26].

A compression curve can be used to visually depict the connection between compression force and displacement. Typically, this curve contains three regions:

Elastic region: When the external compressive force is released, the material deforms elastically in this area, returning to its former shape. In this area, the compression force displacement curve is linear. The cell deforms elastically at modest compression forces, returning to its initial shape once the force is removed. The stiffness of the cell is shown by the slope of the curve in this area [26].

Plastic region: As the compression force develops in this area, the cell deforms plastically, undergoing long-lasting deformation even after the force is removed. The nonlinear curve in this area displays a plateau that corresponds to the material's yield point. The greatest force that the cell can withstand without permanently deforming itself is represented by the curve's yield point [26].

Failure region: The cell will eventually fracture in this location if the compression force is allowed to rise past the yield point. The ultimate compressive strength is a measure of the highest force a cell can withstand before shattering. when a cell fails and fractures as a result of too much stress or distortion. The material's failure point is shown by a sudden drop in the compression force displacement curve to zero [26].

CFD management may affect the lithium-ion cell life cycle. The performance and dependability of the cell may be impacted by excessive compression or unequal compression, Optimum CFD management can increase the effectiveness of heat transfer and cooling, lower the danger of thermal runaway, and lengthen the cycle life of the cell.

One of the most important elements affecting this behavior of the cells is the foams placed between the cells, the mechanical properties of these foams are examined with the graphic shown in Figure 3.6.

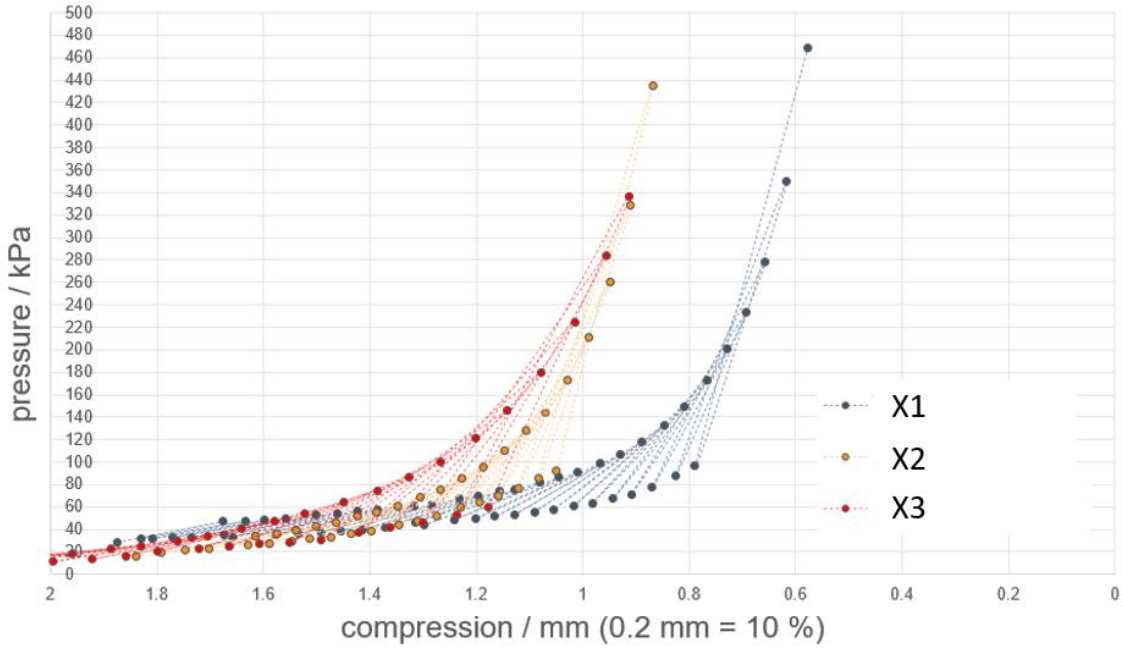

Figure 3.6: CFD curves of foams

For a given 2 mm thickness, the maximum compression values of the foams can be seen in Table 3.3.

Table 3.3: Max. compression values

	X1	**X2**	**X3**
Thickness	2 mm	2 mm	2 mm
Max. compression	71 %	56 %	54 %

3.2.3 Thermal propagation impact

3.2.3.1 Foam x1

Test object

Six cells that were not electrically connected were used as test objects. For this object, Foam X1 was placed on each cell. Cassettes were used to cover the cells as in the original design. Finally, the cell stack was covered with an aluminum housing. The voltage and temperature measurement cables were extracted from the housing and plugged into the data logger to record the test data. The structure and thermocouple locations are shown in Figure 3.7.

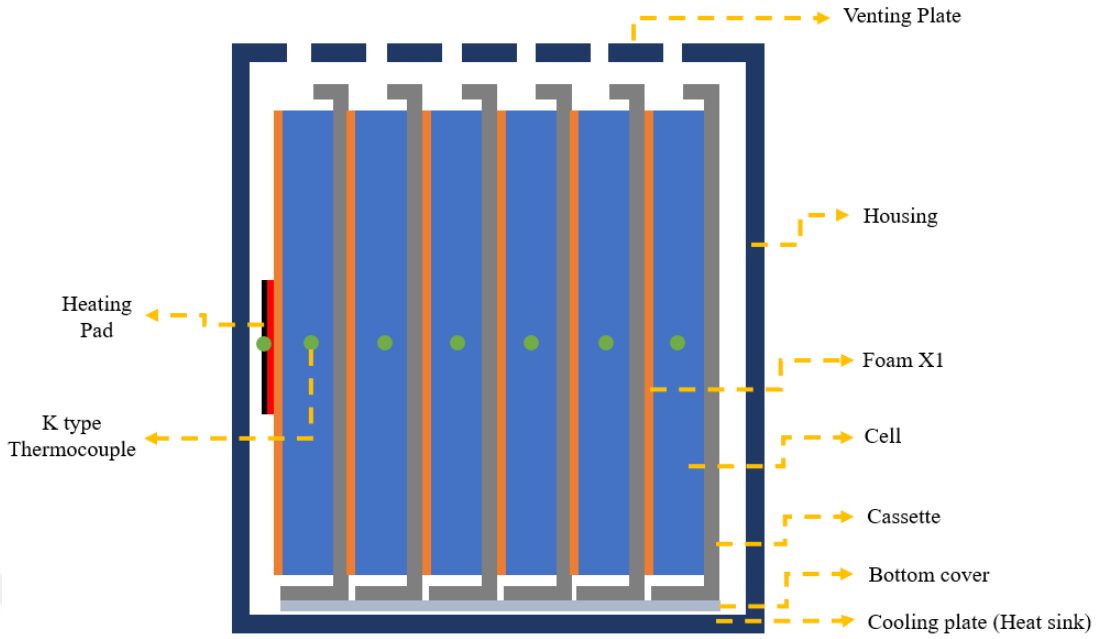

Figure 3.7: Test object sketch for foam X1

Test details

The target was to understand the thermal propagation durations from one cell to the other using foam X1. The test object was placed in a safe environment before the testing. All measurement data and videos were recorded. The heater was powered by an external AC power supply to initiate thermal runaway in a single cell. After approximately 50 s, thermal runaway was observed, after TR, the power of the heating pad was cut off. Thermal propagation continued until all the cells were burnt.

3.2.3.2 Foam x2

Test object

As a test object, six cells that were not electrically connected were used for evaluation. For this setup, X2 foam was located near each cell. The cells were placed in cassettes, and the cell stack was covered with aluminum housing. Voltage measurement cables were extracted and placed into the data logger to log voltage information during the test. Thermocouples were located inside the module in the middle of the cell surfaces and heating pad and then plugged into the data logger to record the temperatures. The structure and thermocouple locations are shown in Figure 3.8.

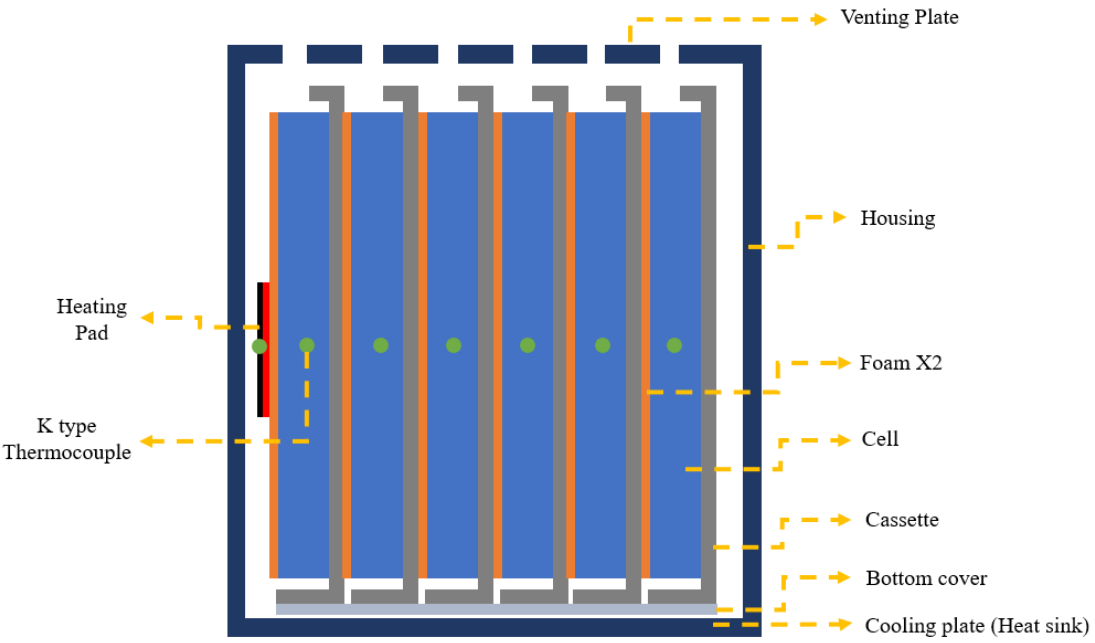

Figure 3.8: Test object sketch for foam X2

Test details

The purpose of this test was to determine the thermal propagation durations from one cell to another using foam X2. The test object was then placed in a safe environment. All measurement data were logged using a datalogger with a 10 ms sampling rate. The test execution was recorded using a video camera along with the temperature and voltage data. At the beginning of the test, the heater was started using an external AC power supply to initiate thermal runaway. Thermal runaway started immediately after approximately 50 s when the heating pad was powered. Once TR was observed, the power of the heating pad was cut off. Thermal propagation continued until all cells were burnt.

3.2.3.3 Foam x3

Test object

The test object was a minimodule containing six individual lithium-ion pouch cells. For this purpose, foam X3 was placed between the cells. The cells were located inside a cassette that formed a cell stack. aluminum housing encapsulated the cell stack. Voltage and temperature measurement cables were extracted from the housing and plugged into the data logger for recording test data. The structure and thermocouple locations are shown in Figure 3.9.

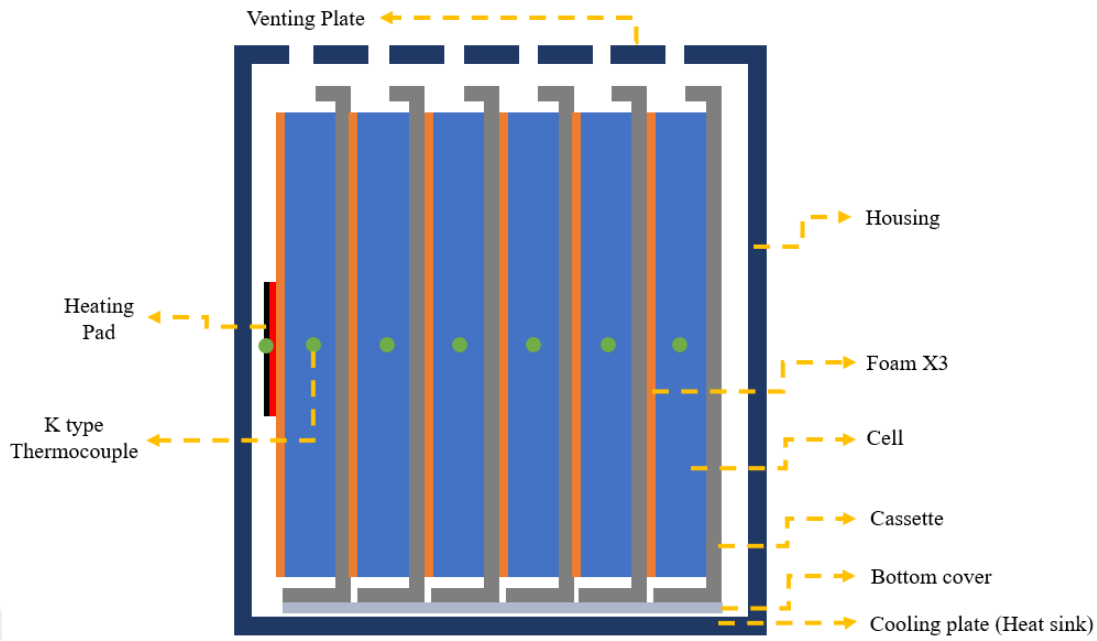

Figure 3.9: Test object sketch for foam X3

Test details

The target was to extract the thermal propagation durations from one cell to the other using foam X3. The test object was placed in a safe environment before the test. All measurement data and video were recorded. The heater was powered by an external AC power supply to initiate thermal runaway in a single cell. After approximately 50 s, a thermal runaway was initiated as follows: the power of the heating pad was cut off. Thermal propagation was observed until all the cells were burnt.

3.3 Optimization Studies for TP Duration on Pack Level

3.3.1 Attempt 1

After foam selection, the pack-level performance had to be understood. A high-voltage battery pack consisting of 108 series and three parallel-connected Li-ion cells was created. In total, 10 modules were utilized in the pack: 8 out of 10 had a configuration of 12S3P, and 2 out of 10 had a configuration of 6S3P. The modules were connected in series to each other, and all modules had their own monitoring circuits to track the cell voltages and temperatures. These circuits were controlled by a master unit inside the pack. Moreover, HV battery packs also include passive protection systems such as fuses and contactors. A representation of the HV battery pack is shown in Figure 3.10.

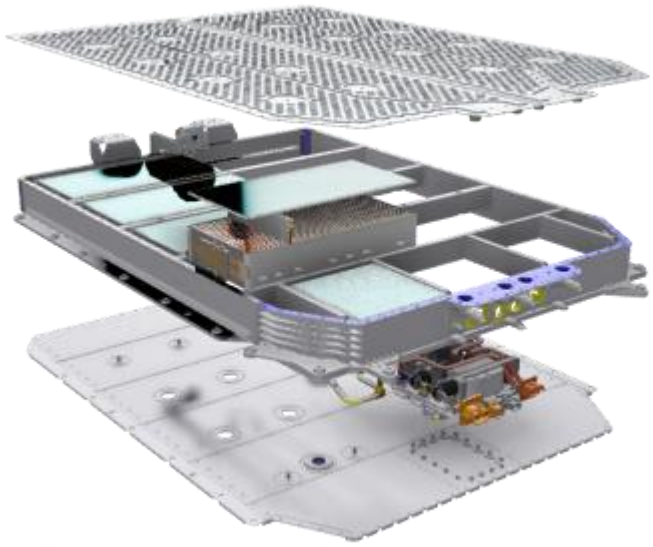

Figure 3.2: A representation of the HV battery pack

3.3.1.1 Test object

The test object was a complete HV battery pack equipped with external thermocouples, voltage-sensing cables, and a heating pad for triggering. The temperature and voltage measurement cables were extracted from the housing and plugged into the data logger to record the test data. Action and thermal cameras were placed around the test specimens. The structure and thermocouple locations were given in Figure 3.11. The sensor details were listed in Table 3.4. Thermocouples measuring up to 1000 °C were used inside the pack. As a trigger point, the first cell of module 2, where the M2 sensor was placed, was selected because the area was close to the electronic parts and had less volume owing to the number of busbars. Therefore, thermocouples were placed around the trigger point. D sensors are located on the modules, whereas the M and S sensors are placed on the side of the modules. P sensor was in the part that consist of battery electronics, lastly, CB sensors were located in the empty areas between the modules. Additionally, there are thermocouples, inside the trigger module, on a heating pad and cells 1, 2, 4, 7,10.

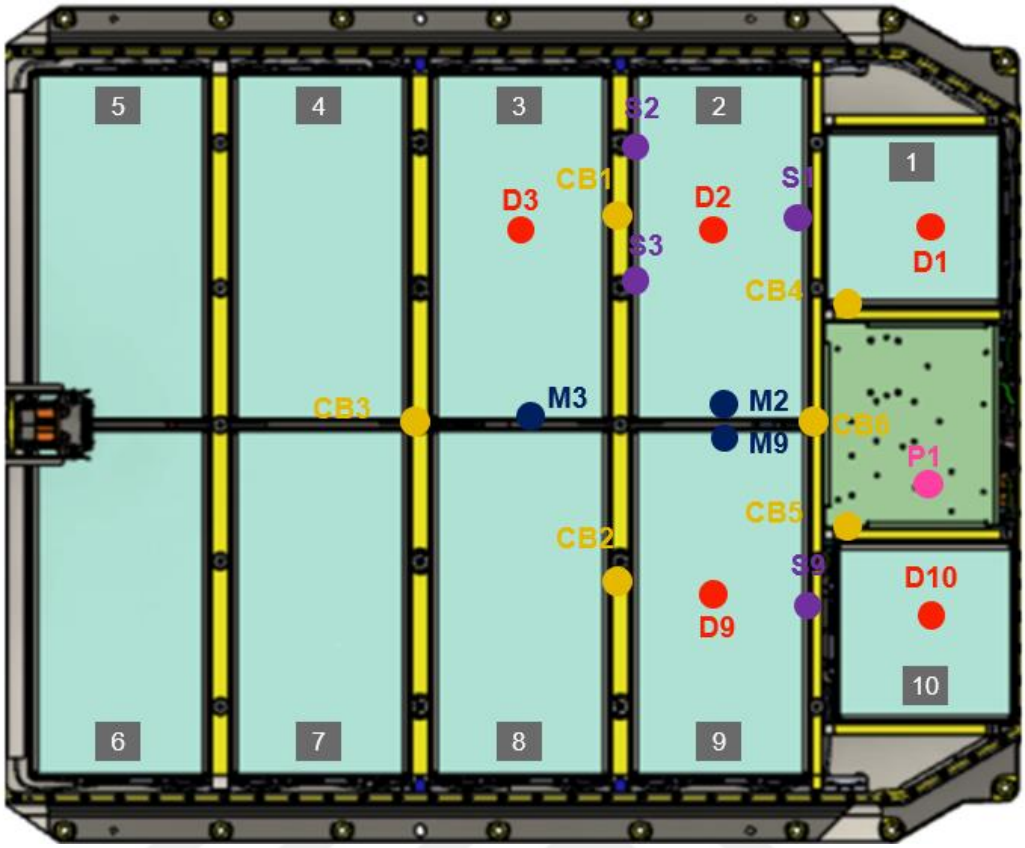

Figure 3.3: Sensor placements for thermal propagation test of the pack

Table 3.4: Sensor descriptions

Sensor	Quantity	Location
D	5	On module
M	3	On end plates of modules
CB	6	On cross beams
S	4	On the side plates of modules
P	1	On fuse
Total	19	

3.3.1.2 Test details

The objective was to understand the thermal propagation performance of the pack and analyze the possible improvement areas. Prior to the testing, the test object was placed in a safe environment. All measurement data from the battery management system, external temperature, and voltage sensors were recorded along with thermal and standard videos. All measurement data were logged via a datalogger using CAN Bus communication. Vector 1640A was used to connect the data logger and the computer. Data were observed using Vector CANoe on a laptop during the test. The heater was powered by an external AC power supply to initiate thermal runaway in a single cell. After around 50 seconds, the thermal runaway was initiated, as follows, the

power of the heating pad was cut off. Thermal propagation was observed until all cells were burned using sensors and cameras. A screenshot of the test computer screen shows how the test was observed from a thermal camera, as shown in Figure 13.

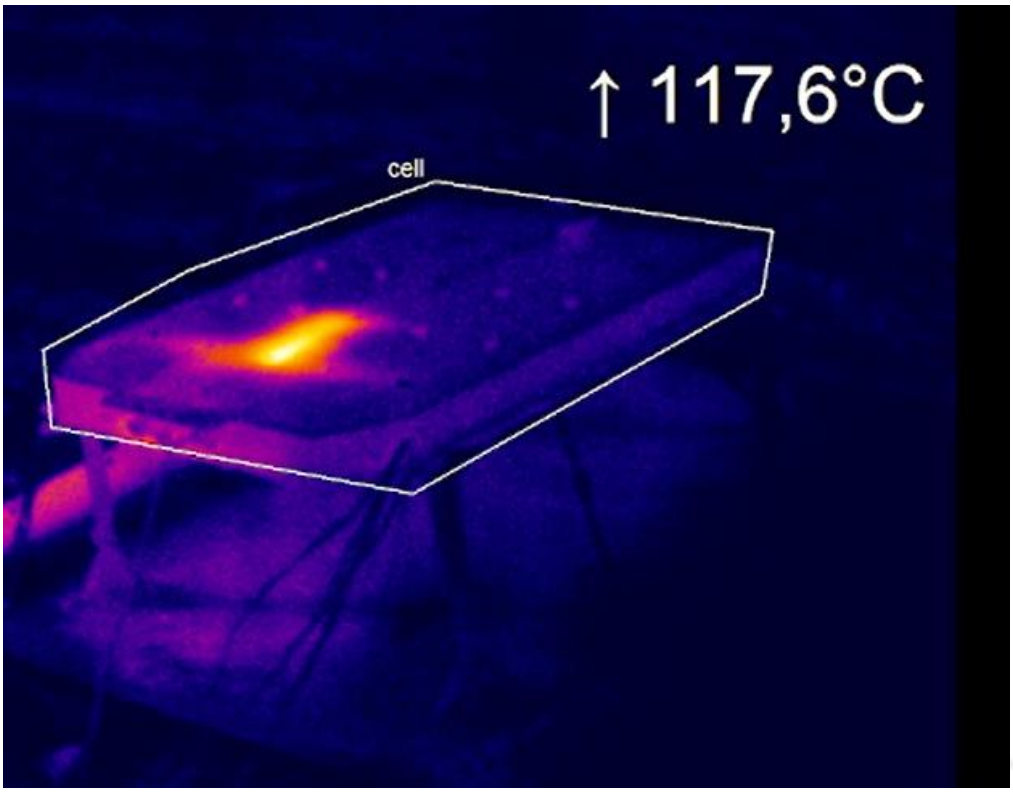

Figure 3.12: Thermal camera observation during the test

3.3.2 Attempt 2

3.3.2.1 Test object

The test item was a complete HV battery pack that includes cables for measuring the voltage, external thermocouples, and a heating pad for triggering.The cables for measuring voltage and temperature were removed from the casing and plugged into the data logger to record the test results. Action and infrared cameras were installed around the test object. The temperature and voltage measurement points were the same as those used in the first test. Additionally, a voltage measurement point was added between the trigger module terminal and its casing to observe the short circuit.

3.3.2.2 Test details

Understanding the measured performance and identifying more potential areas for improvement were the main goals of this test. Prior to the test, the test object was placed in a secure area. Along with the thermal and conventional videos, all measurement information from the BMS and external temperature and voltage sensors were recorded. All measurement data were logged via datalogger using CAN Bus communication. Vector 1640A was used for the connection between the data logger and the computer. Data was observed via Vector CANoe in the test laptop during the test. The heater was activated to initiate the thermal runaway of a single cell by an external AC power source. The electricity to the heating pad was shut off after approximately 50 s when the thermal runaway started. Thermal propagation was monitored using sensors and cameras until all the cells were burnt.

3.3.3 Attempt 3

3.3.3.1 Test object

A complete HV battery pack with cables for measuring the voltage, external thermocouples, and a heating pad for triggering served as the test object. To record the test results, cables for measuring the voltage and temperature were pulled from the shell. Action and infrared cameras were mounted on the test object. The points for measuring the voltage and temperature were the same as in the first and second tests; the only difference was that there was no temperature sensor inside the trigger module. To detect a short circuit, a voltage measurement point was also installed between the terminal and the enclosure of the trigger module.

3.3.3.2 Test details

The major objectives of this test were to comprehend the performance of the measures taken and uncover additional potential areas for improvement. The test object was positioned at a safe location before testing. All measurement data from the BMS and external temperature and voltage sensors were recorded together with thermal and conventional videos. All measurement data were logged via datalogger using CAN Bus communication. Vector 1640A was used for the connection between the data logger and the computer. Data was observed via Vector CANoe in the test laptop during the test. An external AC power supply was turned on the heater to begin

the thermal runaway of a single cell. When thermal runaway began, the current to the heating pad was cut off after approximately 50 s. Thermal propagation was tracked using sensors and cameras until every cell was burned.

4. RESULTS AND DISCUSSIONS

In this chapter, first of all, triggering method test results were given. Then, the results of the thermal propagation impact of the foams were presented. Finally, the test results of the packs were shown. The results were presented as graphs and data tables.

4.1 Comparison of Trigger Methods

4.1.1 Test results of overcharge triggering method

Figure 4.1 shows the temperature values of the first, second, third, fourth, seventh, and tenth cells. The propagation time between the cells was extracted from the data. Observing 10 cell thermal runaway would be enough to have a comparison for evaluation; therefore, the temperature of rest was not tracked. After 10 s, the first cell TR started, and the fire propagated to the second cell and was held for 71 s before jumping to the third cell. The temperature was maintained at approximately 900 °C. The temperature peaks were considered measurement errors. The durations were listed in Table 4.1.

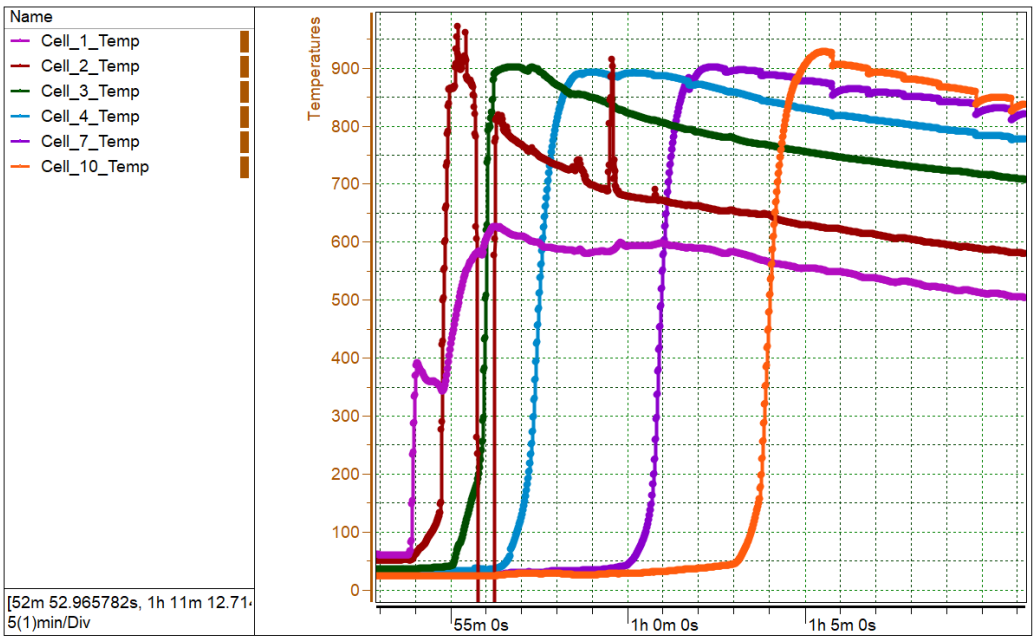

Figure 4.1: Cell temperatures for the overcharge triggering method

Table 4.1: Thermal propagation durations for overcharge triggering method

Propagation	Duration [s]
cell 1 to cell 2	10
cell 2 to cell 3	71
cell 3 to cell 4	93
cell 4 to cell 7	215
cell 7 to cell 10	185

4.1.2 Test results of heating triggering method

Figure 4.2 shows the temperature values of the first, second, third, fourth, seventh and tenth cells. Propagation time between the cells was extracted from the data. The heating pad power was cut off when the TR was observed in the first cell. After 25 s, the first cell TR started, and the fire propagated to the second cell and was held for 58 s before jumping to the third cell. The temperature reached approximately 900 °C. The durations are listed in Table 4.2. Data tracking was concluded after 10 cells were burnt.

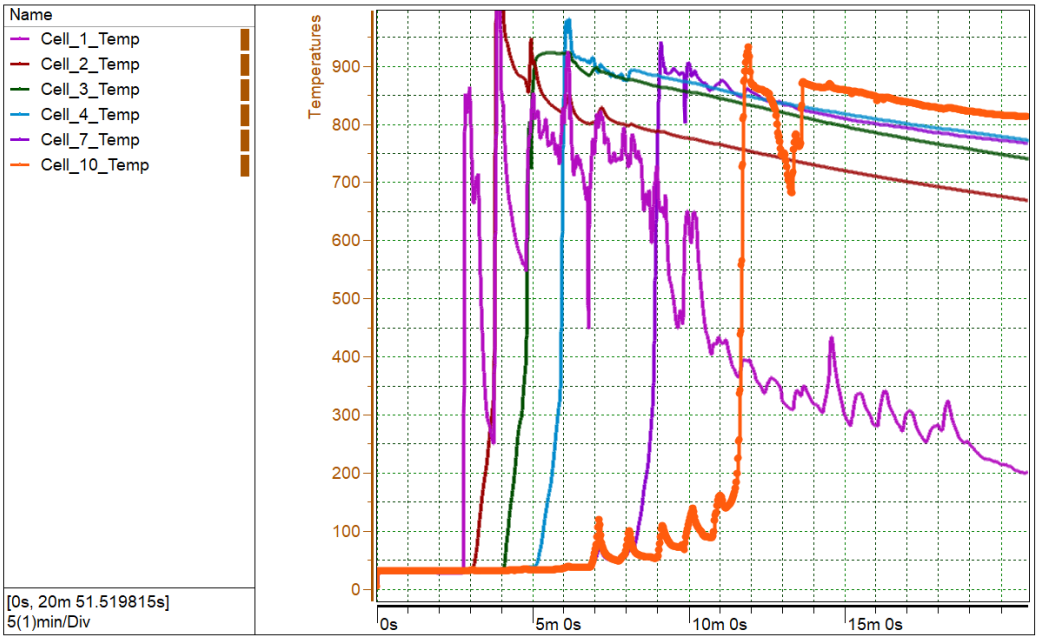

Figure 4.2: Cell temperatures for heating triggering method

Table 4.2: Thermal propagation durations for heating triggering method

Propagation	Duration [s]
cell 1 to cell 2	25
cell 2 to cell 3	58
cell 3 to cell 4	68
cell 4 to cell 7	182
cell 7 to cell 10	175

4.2 Comparison of Foams

4.2.1 Test results of foam x1

Figure 4.3 displays the temperature values for the cells and the heating pad, and Figure 4.4 displays the voltage values for each cell individually. Once the TR started in one cell, the voltage drop started until all electrolytes were dissolved. The thermal propagation durations were calculated by examining the voltage drops. The durations were listed in Table 4.3.

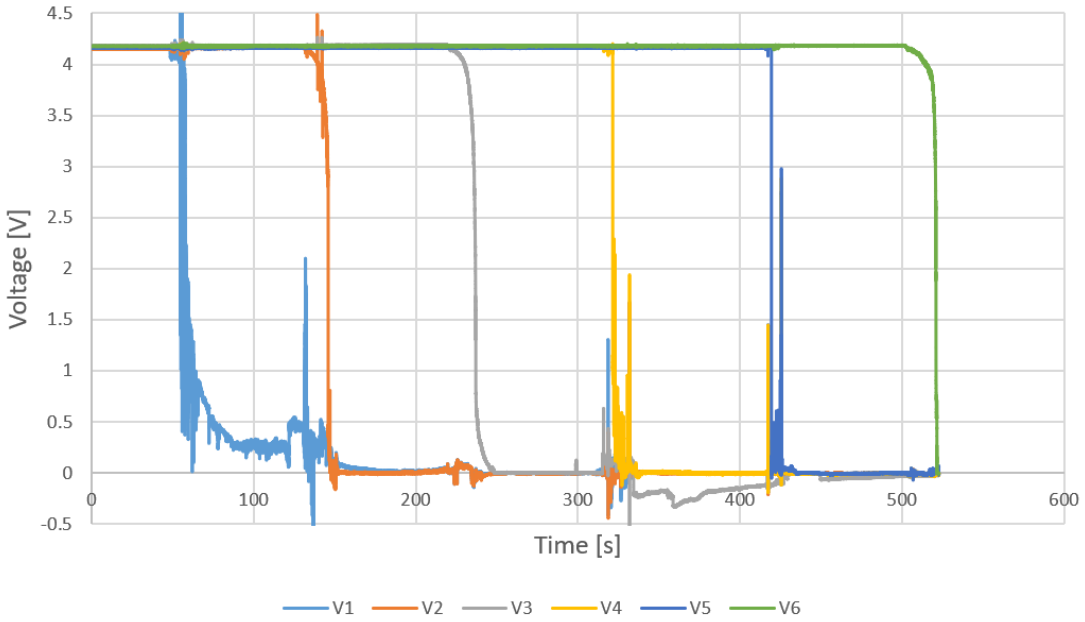

Figure 4.3: Cell voltages for foam X1

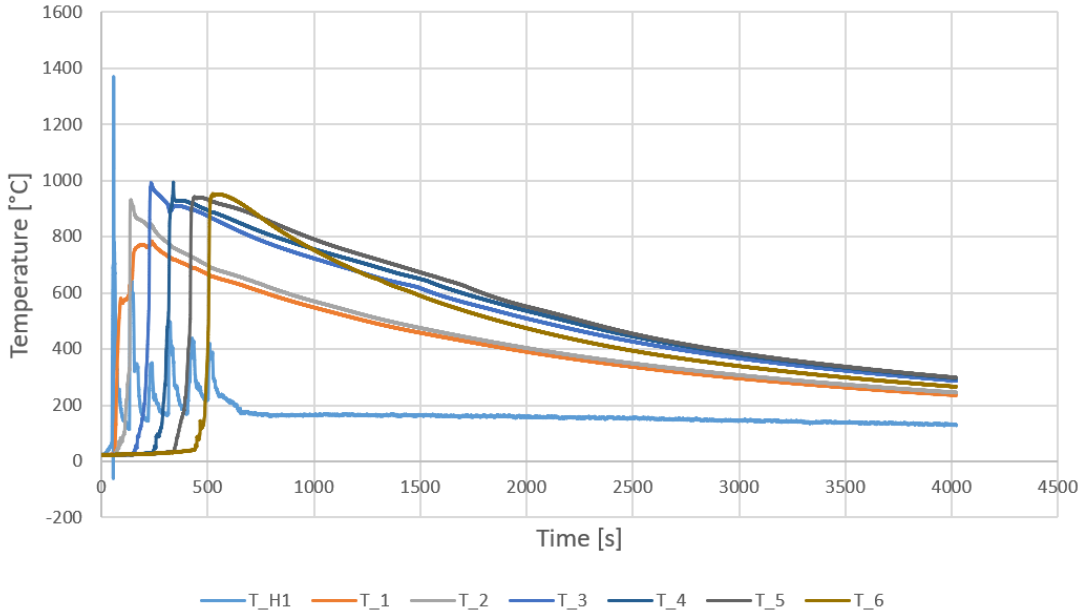

Figure 4.4: Cell temperatures for foam X1

Table 4.3: Thermal propagation durations for foam X1

Propagation	Duration [s]
cell 1 to cell 2	85
cell 2 to cell 3	89
cell 3 to cell 4	96
cell 4 to cell 5	104
cell 5 to cell 6	84
Total Reaction	458

4.2.2 Test results of foam x2

Figure 4.5 shows the voltage values of all cells individually, while Figure 4.6 shows the temperature values of the cells and the heating pad. In this test, temperature measurements of cells 1 and 5 were lost; however, this did not affect the results or evaluation. Durations should be calculated by examining the voltage drop, in which voltage measurements are more reliable than temperature measurements because of the uncontrollable and high-energy reactions. The propagation time between the cells was determined from the voltage data. The durations were listed in Table 4.4.

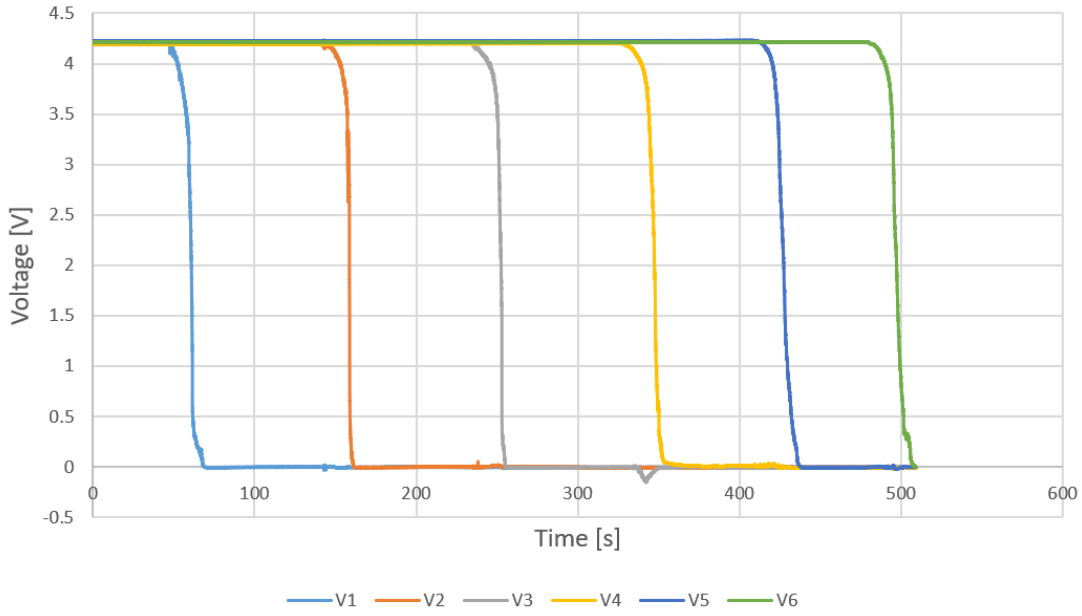

Figure 4.5: Cell voltages for foam X2

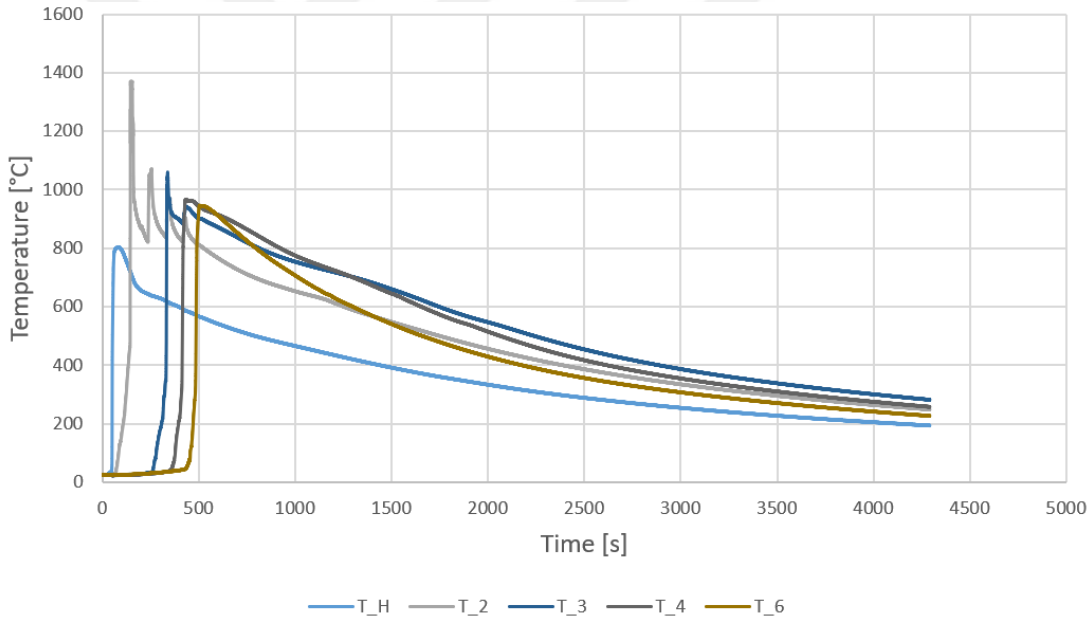

Figure 4.6: Cell temperatures for foam X2

Table 4.4: Thermal propagation durations for foam X2

Propagation	Duration [s]
cell 1 to cell 2	90
cell 2 to cell 3	91
cell 3 to cell 4	96
cell 4 to cell 5	81
cell 5 to cell 6	70
Total Reaction	428

4.2.3 Test results of foam x3

Figure 4.7 shows the voltage values of all cells separately, and Figure 4.8 shows the temperature values of the cells and the heating pad. Once the thermal runaway in one cell started, the fire propagated to the neighboring cells. The duration of thermal propagation between the cells was calculated from the voltage data. The durations were listed in Table 4.5.

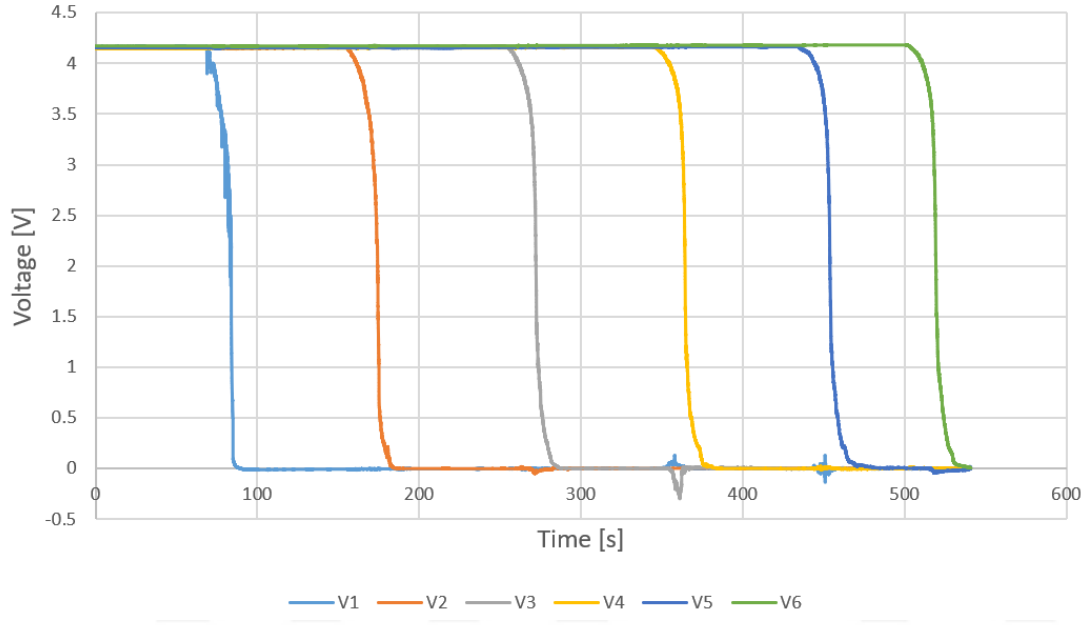

Figure 4.7: Cell voltages for foam X3

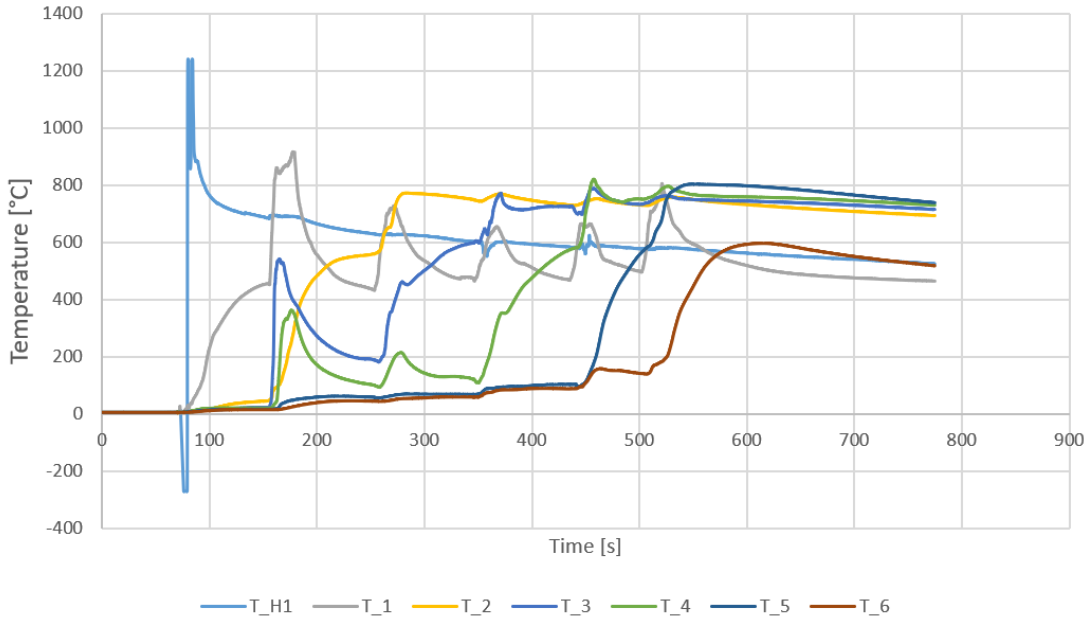

Figure 4.8: Cell temperatures for foam X3

Table 4.5: Thermal propagation durations for foam X3

Propagation	Duration [s]
cell 1 to cell 2	87
cell 2 to cell 3	99
cell 3 to cell 4	92
cell 4 to cell 5	88
cell 5 to cell 6	68
Total Reaction	434

4.3 Pack Level Optimization Attempts

4.3.1 Results of attempt 1

The test failed after a short period. The fire was observed outside the pack. The pass criterion was the observation of fire less than 5 min after the TR started in one cell. After analyses and evaluations, it was determined that a short circuit occurred because of a thermal runaway between the modules. Accordingly, it was decided to place a melting fuse between the modules to prevent short circuits during TP. An electrical diagram of the HV battery pack is shown in Figure 4.9. As shown in Figures 4.10, 4.11, and 4.12, TR started in the neighboring module of the trigger module within a short period. As a result, the duration between the TR start and the appearance of the fire outside the pack was recorded as T min.

In addition, it should be understood that the probability of spontaneous TR in an individual Li-ion cell is low, with approximately one in tens of millions of TR events leading to battery fires and explosions [27].

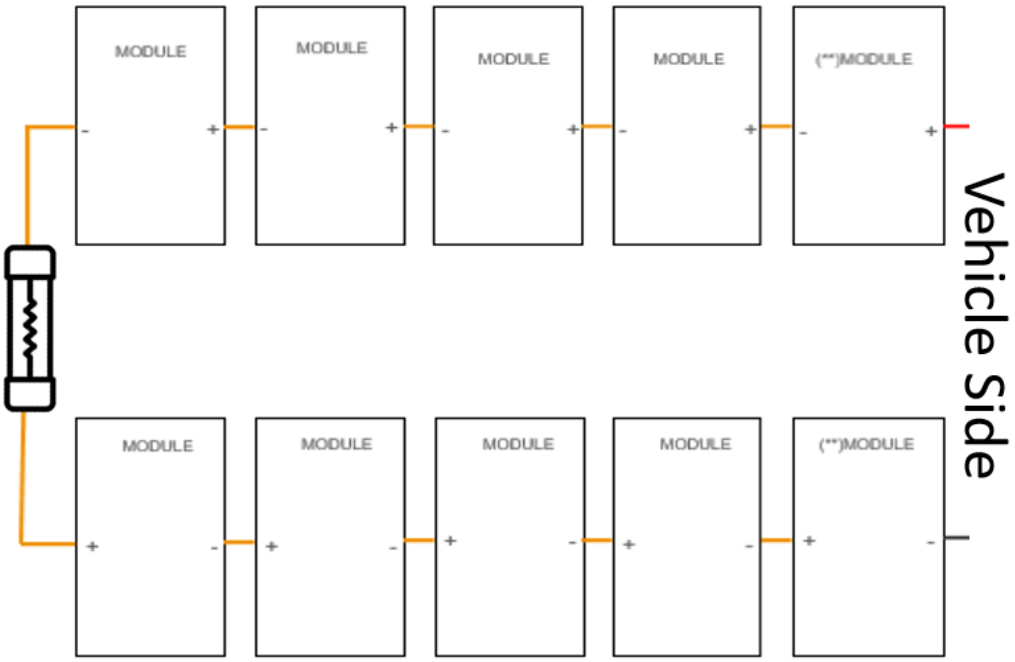

Figure 4.9: Electrical diagram of the pack

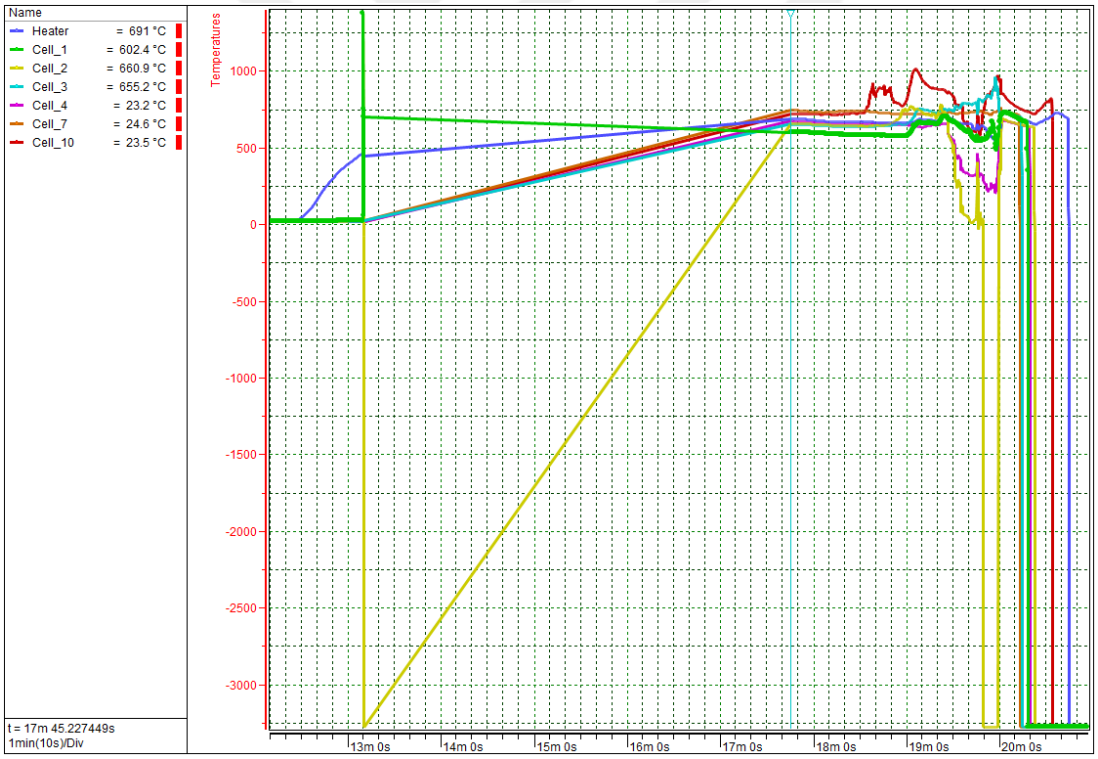

Figure 4.10: Trigger module cell temperatures

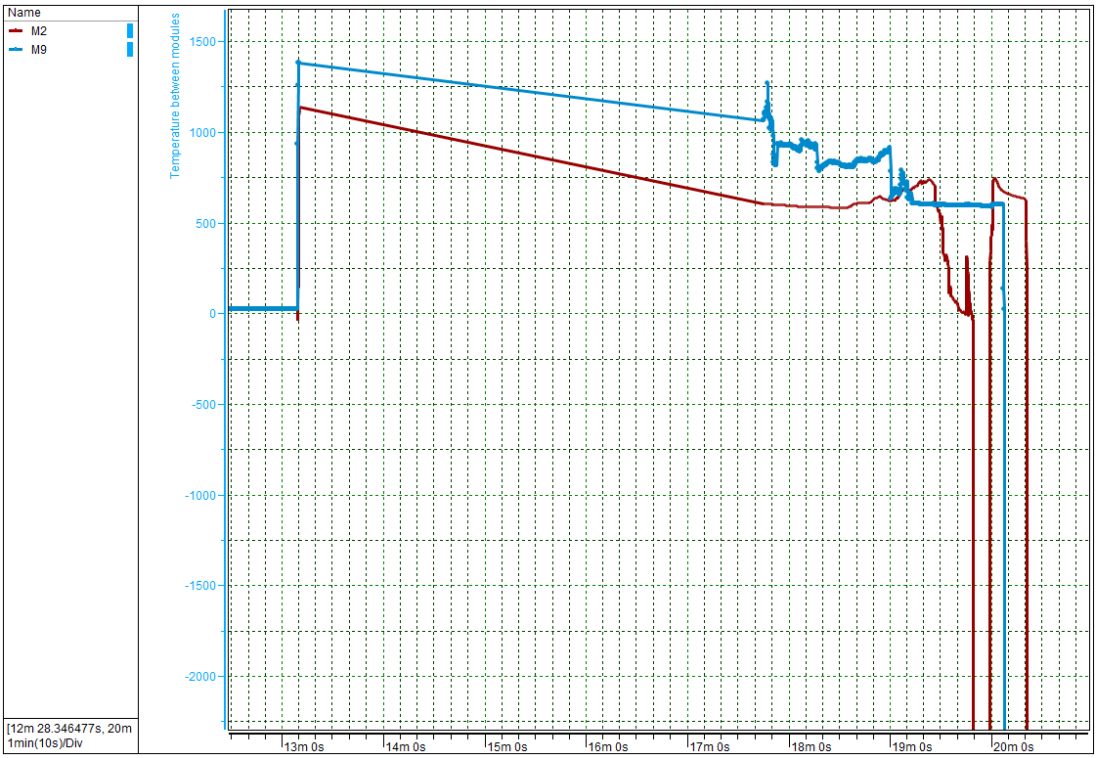

Figure 4.11: Trigger module and neighboring module temperatures of attempt 1

Figure 4.12: Trigger module and neighboring module voltages of attempt 1

4.3.2 Results of attempt 2

The addition of fuse between the modules worked well, TP performance improved four times, and the duration between the TR start and the appearance of fire outside the pack was recorded as 4T min. In Figure 4.13, it can be seen that after TR started, a voltage was observed between the trigger module terminal and its enclosure, and the fuse acted quickly and cut the electrical connection between the modules in half. Therefore, the catastrophic effects of short circuits were prevented. In "Investigating the relationship between internal short circuit and thermal runaway of lithium-ion batteries under thermal abuse condition", the effect of the internal short circuit to thermal propagation was highlighted [28]. Data were analyzed, and the propagation durations between cells and modules were calculated from the data, as shown in Table 4.6. The graphs for trigger module cell temperatures, trigger, and neighboring module temperatures, and voltages can be seen in Figures 4.14, 4.15, 4.16, and 4.17. When the thermal and action camera records were analyzed, the gas flow was observed. According to the evaluations, the gas was stuck in a small area and could not be exhausted by the venting valves. Therefore, a pressure build-up occurred. The ideal gas law states that if the pressure increases in a fixed volume, then the temperature in other words energy increases. Consequently, the thermal propagation reaction speed increased. In conclusion, it was determined that the HV busbar routing of the pack was changed. The logic behind the routing change is to create a clear gas flow path. A representation of the routing change is shown in Figure 4.13.

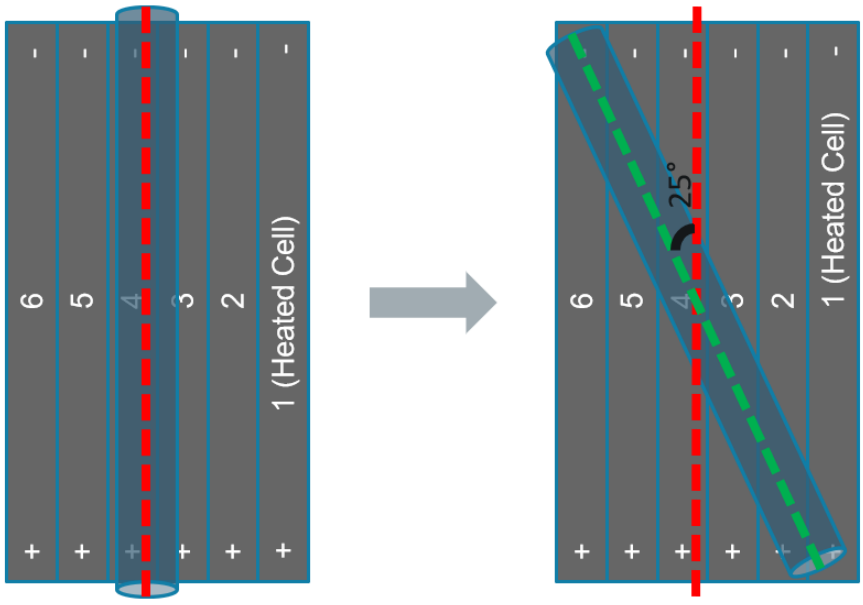

Figure 4.13: Representation of busbar routing change

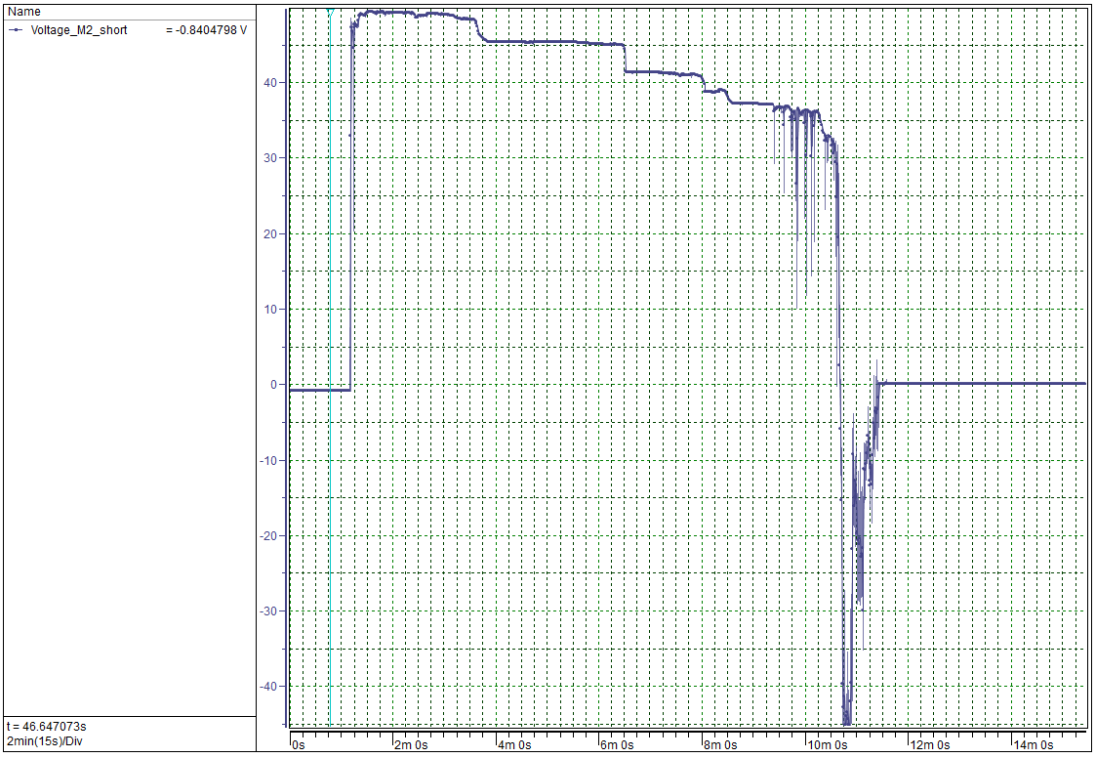

Figure 4.14: Short circuit detection sensor for attempt 2

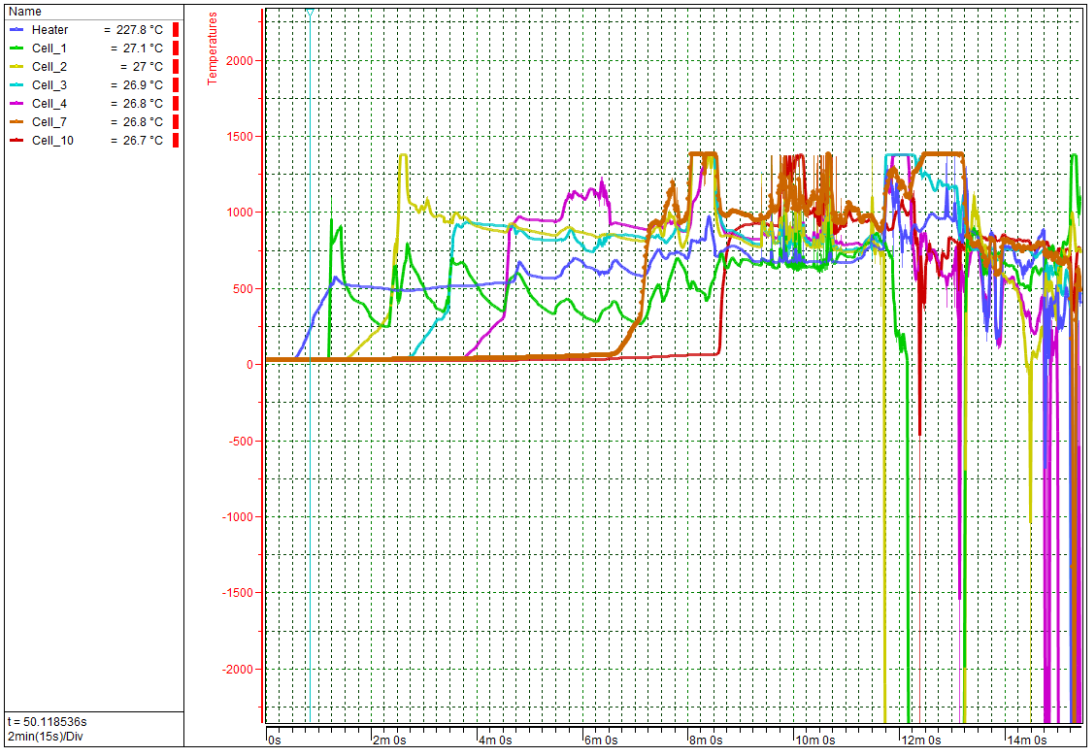

Figure 4.15: Trigger module cell temperatures of attempt 2

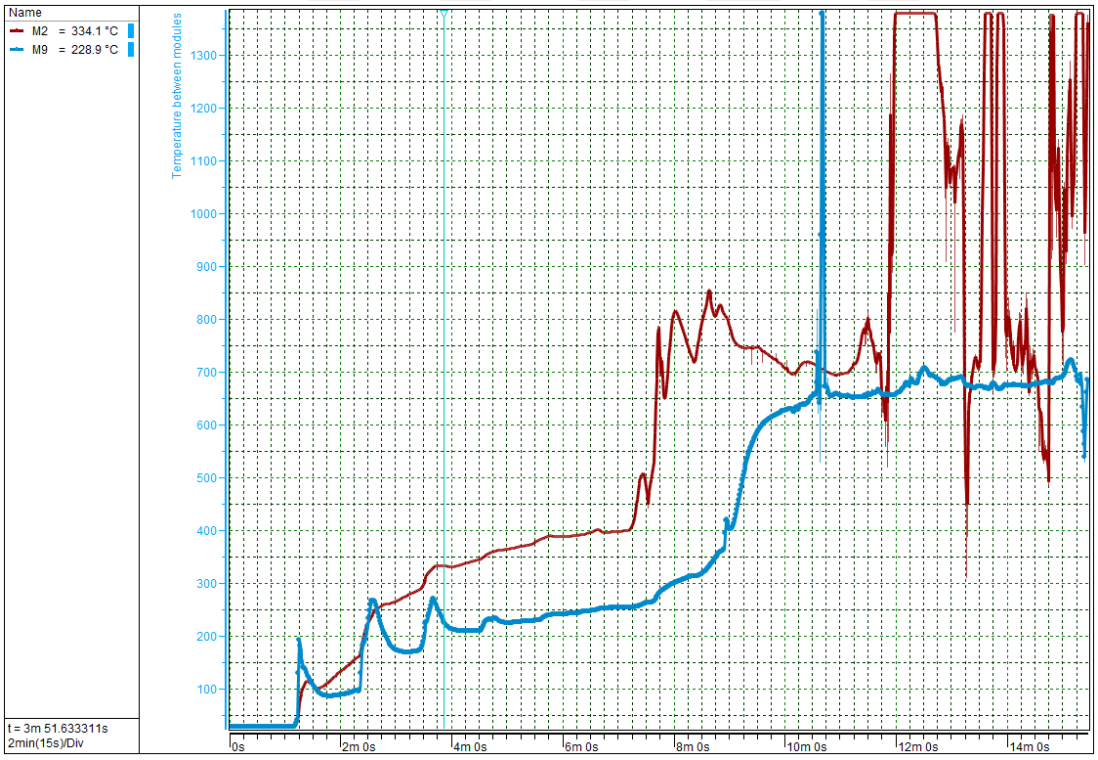

Figure 4.16: Trigger module and neighboring module temperatures of attempt 2

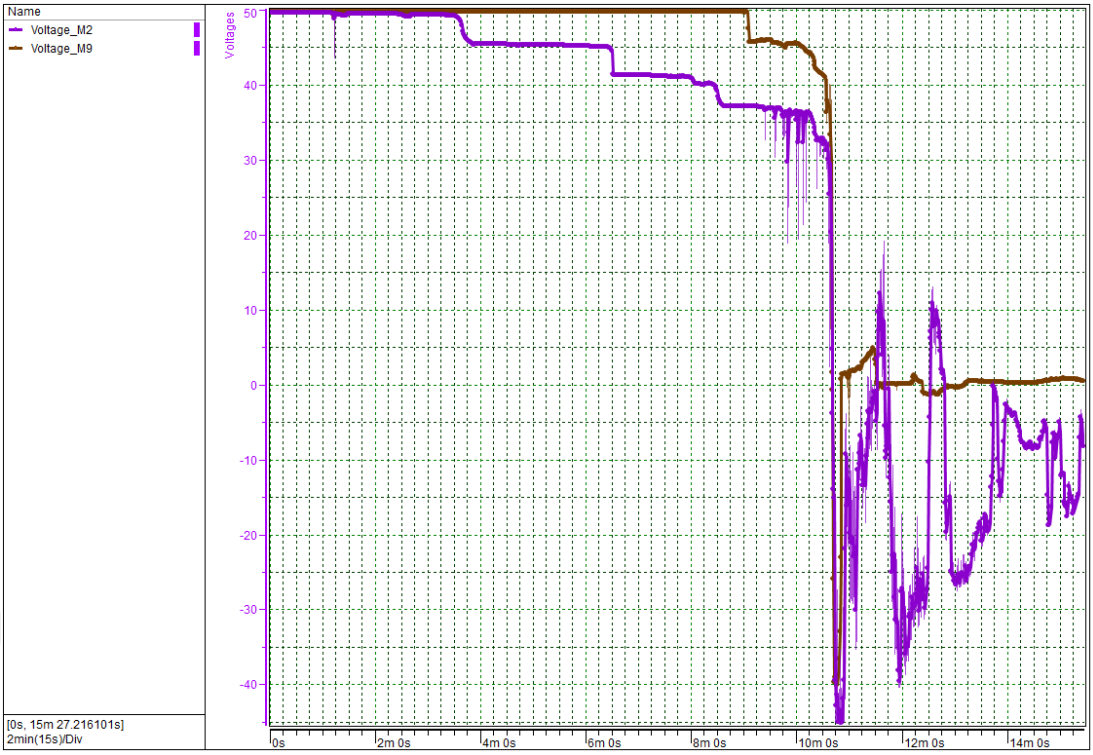

Figure 4.17: Trigger module and neighboring module voltages of attempt 2

Table 4.6: TP Statistics for attempt 2

Time	TP12 (s)	Comment
cell1 to cell2	55	
cell2 to cell3	60	The onset temperature 200 degree
cell3 to cell4	68	
cell4 to cell7	162	
cell7 to cell10	96	
M2 4V decrease	198	4.2 V – 3 parallel cell group
M2 8V decrease	360	
M2 12V decrease	482	
M2 16V decrease	500	
M2 20V decrease	-	
M2 24V decrease	-	
M2 28V decrease	-	
Reaction Speed (Capacity/s)	0.031	
M9 4V decrease	494	4.2 V – 3 parallel cell group
M9 8V decrease	-	
M9 12V decrease	-	
Reaction Speed (Capacity/s)		
Fire Time	**4T**	

4.3.3 Results of attempt 3

Changing the HV busbar routing and creating a gas flow extended the duration of the thermal propagation. results were recorded at 6T. In Figure 4.18, a short circuit was observed again, and the fuse acted in the same manner. The graphs for the trigger and neighboring module temperatures and voltages are shown in Figures 4.19 and 4.20, respectively. The durations were listed in Table 4.7.

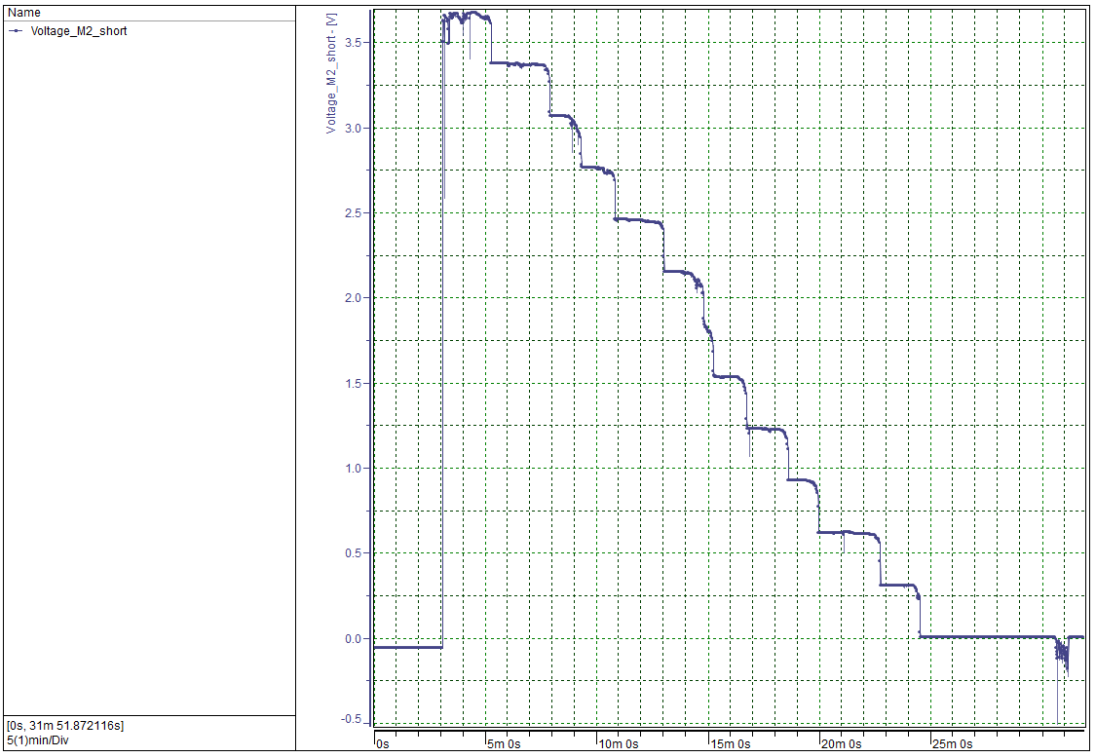

Figure 4.18: Short circuit detection sensor for attempt 3

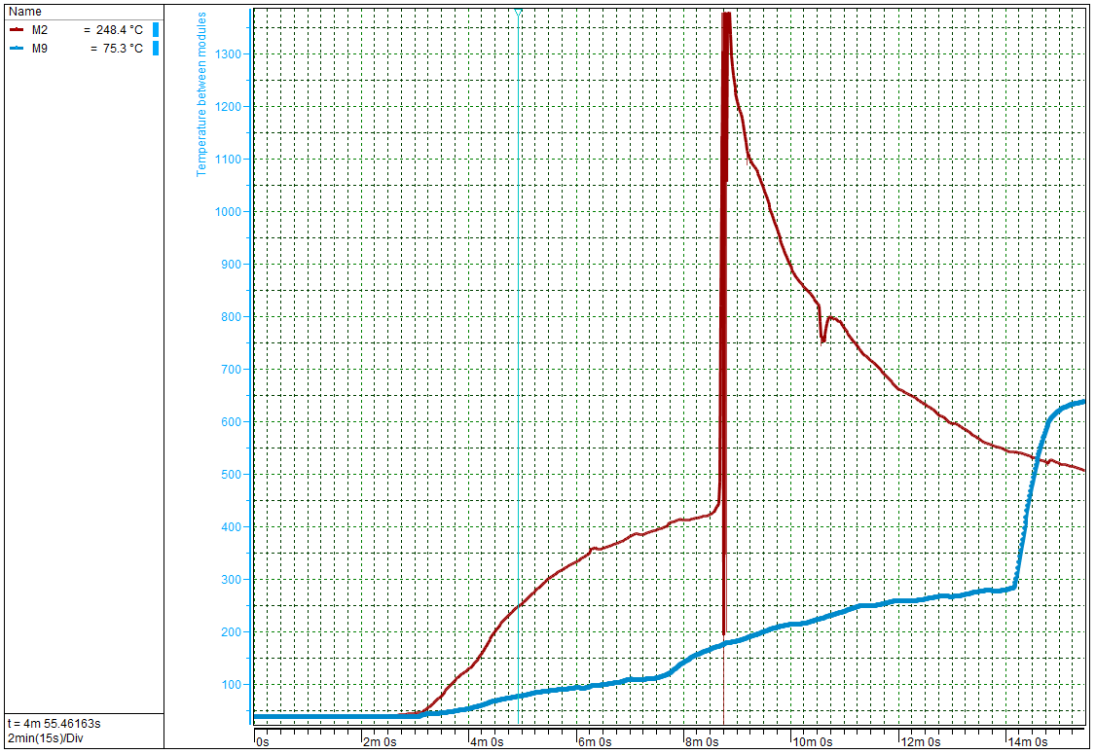

Figure 4.19: Trigger module and neighboring module temperatures of attempt 3

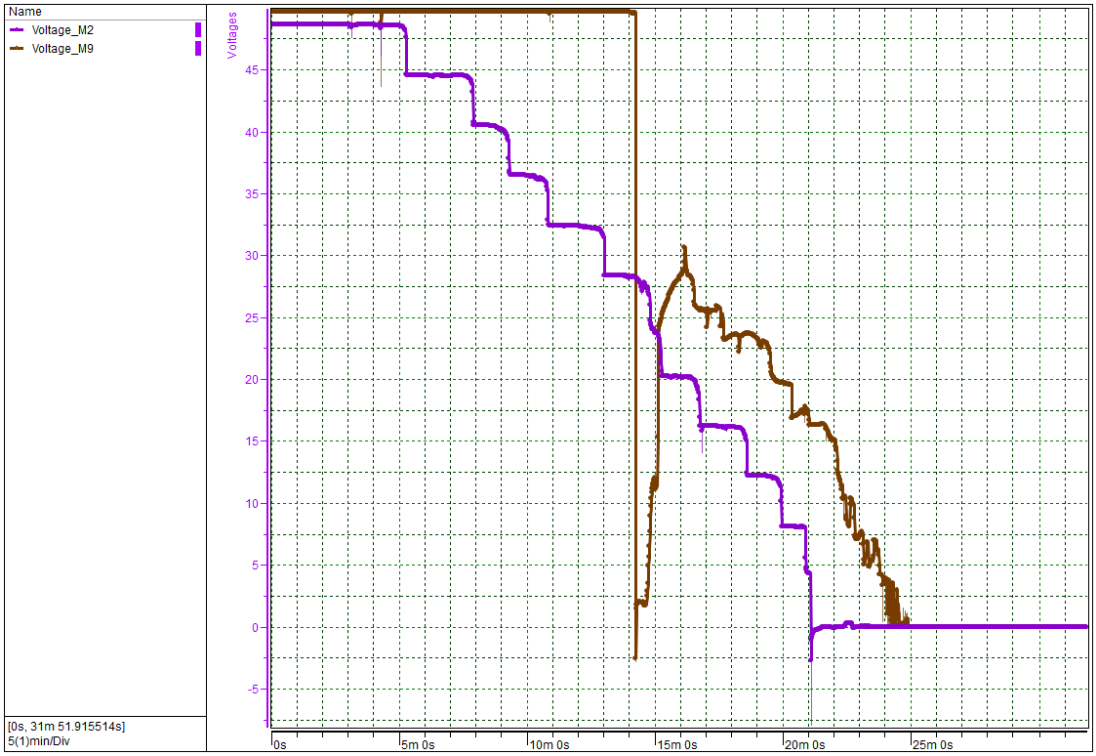

Figure 4.20: Trigger module and neighboring module voltages of attempt 3

Table 4.7: TP statistics for attempt 3

Time	Attempt 3	Comment
cell1 to cell2		
cell2 to cell3		The onset
cell3 to cell4	no temperature sensor	temperature
cell4 to cell7		200 degree
cell7 to cell10		
M2 4V decrease	216	4.2 V – 3 parallel
M2 8V decrease	375	cell group
M2 12V decrease	460	
M2 16V decrease	547	
M2 20V decrease	680	
M2 24V decrease	788	
M2 28V decrease	820	
Reaction Speed (Capacity/s)	0.022	
M9 4V decrease	no voltage decrease	4.2 V – 3 parallel
M9 8V decrease	until 761 seconds.	cell group
M9 12V decrease	Then harness	
Reaction Speed (Capacity/s)	damaged	
Fire Time (min)	**6T**	

5. CONCLUSION

5.1 Review & Evaluation

The study began by determining the thermal runaway trigger method, and three different silicon-based foams were evaluated in terms of their compression force displacement effect, thermal conductivity, and thermal propagation effect. The optimal foam was selected after conducting three tests and evaluations. Subsequently, the HV battery pack thermal propagation performance was intended to be understood and three tests were executed.

As can be seen from Table 5.1, there was no significant difference between the tested trigger methods at the module level. However, during overcharging, the neighboring cell of the trigger cell was heated slightly; therefore, this might have affected the results at the pack level. On the other hand, the triggering time was rather long during discharging compared with that of the heating pad. In addition, the heating method is more representative than the overcharging method because, in real life, TR occurs suddenly in the case of an internal short circuit. Furthermore, the BMS always protects the system from failures, such as overcharging.

Table 5.1: Thermal propagation durations for overcharge and heating pad

Propagation	Overcharge Duration [s]	Heating Pad Duration [s]
cell 1 to cell 2	10	25
cell 2 to cell 3	71	58
cell 3 to cell 4	93	68
cell 4 to cell 7	215	182
cell 7 to cell 10	185	175

Product X1 was selected as the optimal foam for the life cycle and safety. Even if it is not the best choice regarding its thermal conductivity value, the CFD curve and TP performance indicate that it should be chosen for the design. As shown in Table 5.2, X1 provides the longest TP duration.

Table 5.2: Thermal propagation durations for foams

	X1	X2	X3
Propagation	**Duration [s]**	**Duration [s]**	**Duration [s]**
cell 1 to cell 2	85	90	87
cell 2 to cell 3	89	93	98
cell 3 to cell 4	96	97	91
cell 4 to cell 5	104	81	87
cell 5 to cell 6	84	70	68
Total Reaction	458	428	434

In conclusion, the propagation performance was enhanced by six times, and the UN ECE R100 regulation requirement, which states that the REESS or vehicle system shall provide a signal to activate the warning indication in the vehicle to allow egress or 5 minutes prior to the presence of a hazardous situation inside the passenger compartment caused by thermal propagation, which is triggered by an internal short circuit leading to a single-cell thermal runaway such as fire, explosion, or smoke was overly achieved. The overall comparative results are presented in Table 5.3.

Table 5.3: TP statistics for attempts 1-3

Time	Attempt 1	Attempt 2	Attempt 3	Comment
cell1 to cell2	N/A	55		
cell2 to cell3		60	no	The onset
cell3 to cell4		68	temperature	temperature
cell4 to cell7		162	sensor	200 degree
cell7 to cell10		96		
M2 4V decrease		198	216	4.2 V – 3
M2 8V decrease		360	375	parallel cell
M2 12V decrease		482	460	group
M2 16V decrease		500	547	
M2 20V decrease		-	680	
M2 24V decrease		-	788	
M2 28V decrease		-	820	
Reaction Speed (Capacity/s)		0.031	0.022	
M9 4V decrease		494	no voltage	4.2 V – 3
M9 8V decrease		-	decrease	parallel cell
M9 12V decrease		-	until 761	group
Reaction Speed (Capacity/s)			seconds. Then harness damaged	
Fire Time (min)	**T**	**4T**	**6T**	

5.2 Future Works

In future work, more methods and materials will be investigated to improve the thermal propagation performance. The ultimate goal is to provide zero thermal propagation. The design shall be done so that fire starts and energy is released without propagating to the neighboring cells.

REFERENCES

[1] Zubi, G., Dufo-López, R., Carvalho, M., & Pasaoglu, G. (2018). The lithium-ion battery: State of the art and future perspectives. *Renewable and Sustainable Energy Reviews, 89*, 292-308.

[2] Nzereogu, P. U., Omah, A. D., Ezema, F. I., Iwuoha, E. I., & Nwanya, A. C. (2022). Anode materials for lithium-ion batteries: A review. *Applied Surface Science Advances, 9*, 100233.

[3] Barré, A., Deguilhem, B., Grolleau, S., Gérard, M., Suard, F., & Riu, D. (2013). A review on lithium-ion battery ageing mechanisms and estimations for automotive applications. *Journal of Power Sources, 241*, 680-689.

[4] Feng, X., Ouyang, M., Liu, X., Lu, L., Xia, Y., & He, X. (2018). Thermal runaway mechanism of lithium ion battery for electric vehicles: A review. *Energy Storage Materials, 10*, 246-267.

[5] Linden, D. and Reddy, T. B. (2002). Handbook of batteries, McGraw-Hill.; Berndt, D. (1993). A Handbook of Battery Technology, Research Studies Press.; Dell, R. M. and Rand, D. A. J. (2001). Understanding batteries, *Royal Society of Chemistry (Great Britain)*

[6] Berndt, D. (1993). A Handbook of Battery Technology, Research Studies Press.; Dell, R. M. and Rand, D. A. J. (2001). Understanding batteries, *Royal Society of Chemistry (Great Britain)*

[7] Xiao, J., Li, X., Tang, M.K., Long, M., Chen, M.J., Wang, M.D., Gao, M.H., Liu, H. (2021). Enhanced electrochemical performance of Li-rich cathode material for lithium-ion batteries, *ICE Publishing*

[8] Mekonnen, Y., Sundararajan, A., & Sarwat, A. I. (2016). A review of cathode and anode materials for lithium-ion batteries. *SoutheastCon 2016*, 1-6.

[9] Loganathan, M. K., Mishra, B., Tan, C. M., Kongsvik, T., & Rai, R. N. (2021). Multi-Criteria decision making (MCDM) for the selection of Li-Ion batteries used in electric vehicles (EVs). *Materials Today: Proceedings, 41*, 1073-1077.

[10] Kalhoff, J., Eshetu, G. G., Bresser, D., & Passerini, S. (2015). Safer electrolytes for lithium-ion batteries: state of the art and perspectives. *ChemSusChem, 8*(13), 2154-2175.

[11] Zhang, L., Li, X., Yang, M., & Chen, W. (2021). High-safety separators for lithium-ion batteries and sodium-ion batteries: advances and perspective. *Energy Storage Materials, 41*, 522-545.

[12] De Hoog, J., Fleurbaey, K., Nikolian, A., Timmermans, J. M., Omar, N., Van Mierlo, J., & Van den Bossche, P. (2014, December). Aging phenomena for Lithium-Ion batteries. In *European Electric Vehicle Congress Brussels, Belgium, 3rd–5th December.*

[13] Danzer, M. A., Liebau, V., & Maglia, F. (2015). Aging of lithium-ion batteries for electric vehicles. *In Advances in battery technologies for electric vehicles* (pp. 359-387). Woodhead Publishing.

[14] Guo, J., Li, Y., Pedersen, K., & Stroe, D. I. (2021). Lithium-ion battery operation, degradation, and ageing mechanism in electric vehicles: an Overview. *Energies, 14*(17), 5220.

[15] Li, Y., Liu, X., Wang, L., Feng, X., Ren, D., Wu, Y., ... & Ouyang, M. (2021). Thermal runaway mechanism of lithium-ion battery with LiNi0. 8Mn0. 1Co0. 1O2 cathode materials. *Nano Energy*, *85*, 105878.

[16] Feng, X., Ouyang, M., Liu, X., Lu, L., Xia, Y., & He, X. (2018). Thermal runaway mechanism of lithium ion battery for electric vehicles: A review. *Energy Storage Materials*, *10*, 246-267.

[17] Feng, X., Ren, D., He, X., & Ouyang, M. (2020). Mitigating thermal runaway of lithium-ion batteries. *Joule*, *4*(4), 743-770.

[18] Zhang, W., Liang, Z., Yin, X., & Ling, G. (2021). Avoiding thermal runaway propagation of lithium-ion battery modules by using hybrid phase change material and liquid cooling. *Applied Thermal Engineering*, *184*, 116380.

[19] Yang, X., Duan, Y., Feng, X., Chen, T., Xu, C., Rui, X., ... & Gao, S. (2020). An experimental study on preventing thermal runaway propagation in lithium-ion battery module using aerogel and liquid cooling plate together. *Fire technology*, *56*, 2579-2602.

[20] Huang, L., Zhang, Z., Wang, Z., Zhang, L., Zhu, X., & Dorrell, D. D. (2019). Thermal runaway behavior during overcharge for large-format Lithium-ion batteries with different packaging patterns. *Journal of Energy Storage*, *25*, 100811.

[21] Lai, X., Wang, S., Wang, H., Zheng, Y., & Feng, X. (2021). Investigation of thermal runaway propagation characteristics of lithium-ion battery modules under different trigger modes. *International Journal of Heat and Mass Transfer*, *171*, 121080.

[22] Underwriters Laboratories. "UL 9540A Test Method". Access Date: 12.07.2023. https://l24.im/7UyFsg

[23] The United Nations Economic Commission for Europe (UNECE). "UN ECE R100 Rev.3: Uniform provisions concerning the approval of vehicles with regard to specific requirements for the electric power train". Access Date: 12.07.2023. https://l24.im/YeovyIV

[24] The United Nations Global Technical Regulations (UNGTR). "UN GTR No.20 Electric Vehicle Safety (EVS)". Access Date: 12.07.2023. https://l24.im/WTInh

[25] White, G., Hales, A., Patel, Y., & Offer, G. (2022). Novel methods for measuring the thermal diffusivity and the thermal conductivity of a lithium-ion battery. *Applied Thermal Engineering*, *212*, 118573.

[26] Kermani, G., & Sahraei, E. (2017). Characterization and modeling of the mechanical properties of lithium-ion batteries. *Energies*, *10*(11), 1730.

[27] Srinivasan, R., Thomas, M. E., Airola, M. B., Carkhuff, B. G., Frizzell-Makowski, L. J., Alkandry, H., ... & Demirev, P. A. (2020). Preventing cell-to-cell propagation of thermal runaway in lithium-ion batteries. Journal of the Electrochemical Society, 167(2), 020559.

[28] Ren, D., Feng, X., Liu, L., Hsu, H., Lu, L., Wang, L., ... & Ouyang, M. (2021). Investigating the relationship between internal short circuit and thermal runaway of lithium-ion batteries under thermal abuse condition. Energy Storage Materials, 34, 563-573.

CURRICULUM VITAE

Name Surname **:** Kadir ARAS

EDUCATION:

- **B.Sc.** **:** 2018, Istanbul Technical University, Faculty of Electrical and Electronics Engineering, Department of Electrical Engineering

PROFESSIONAL EXPERIENCE AND REWARDS:

- Battery Development Engineer, AVL Turkey, 2018-2020
- Battery Development Engineer, TOGG, 2020-2022
- Battery Development Engineer, Siro Energy, 2022-Ongoing